Linkages between East China Sea Deep-sea Oxygenation and the Variability of the East Asian Summer Monsoon and Kuroshio Current over last 400,000 years

N. Vats[1]*, R. K. Singh[1]*, M. Das[1], A. Holbourn[2], A. K. Gupta[3], S. J. Gallagher[4] and D. K. Pandey[5]

[1]School of Earth, Ocean and Climate Sciences, Indian Institute of Technology Bhubaneswar, Argul, Jatni – 752050, India.

[2]Institute of Geosciences, Christian-Albrechts-University of Kiel, Ludewig-Meyn-Str. 14, D-24118 Kiel, Germany.

[3]Department of Geology and Geophysics, Indian Institute of Technology Kharagpur, Kharagpur – 721302, India

[4]School of Earth Sciences, University of Melbourne, Melbourne, Australia.

[5]ESSO-National Centre for Polar and Ocean Research, Goa - 403804, India.

*Corresponding author: Nishant Vats (nv11@iitbbs.ac.in)

Raj Kumar Singh (rksingh@iitbbs.ac.in)

Key Points:

- Four different phases of bottom water oxygenation prevailed in the East China Sea during the last 400 kyr.
- East Asian Summer Monsoon and Kuroshio Current influence East China Sea productivity, organic export flux and bottom water oxygenation.
- Precessional variability modulates bottom water oxygenation in ECS

Abstract

The East China Sea (ECS) seasonally receives a high organic input due to the terrestrial organic matter influx, which is controlled by the East Asian Summer Monsoon (EASM), and from increased productivity due to upwelling of the subsurface Kuroshio Current (KC). Changes in benthic foraminiferal assemblage composition in combination with paleoceanographic proxy data ($CaCO_3$ (%), TOC (%), $\delta^{13}C_{pf}$, and $\delta^{18}O_{bf}$) are used to reconstruct bottom water oxygenation and organic export flux variability over the last 400 kyr in the ECS. Multivariate analyses of benthic foraminiferal census data identified six biofacies characteristic of varying environmental conditions. These results suggest enhanced EASM precipitation and KC upwelling directly influenced bottom water oxygen content and organic export flux in the ECS. The ECS bottom water was suboxic from MIS (Marine Isotope Stage) 11 to 8; suboxic to dysoxic between MIS 7 and 6, strongly dysoxic between mid-MIS 5 and 4, and exhibited high variability between MIS 3 and 1. Spectral analysis of abundance variations of the representative genera *Quinqueloculina* (oxic), *Bulimina* (suboxic), and *Globobulimina* (dysoxic) reveals a robust 23 kyr signal, which we attribute to precessionally-paced changes in surface productivity and bottom water oxygenation related to EASM and KC variability over the past 400 kyr.

Keywords: IODP Site U1429**,** Bottom water oxygenation**,** Precessional variability, East China Sea, Benthic foraminifera

1 Introduction

The amount of dissolved oxygen in the ocean is affected by numerous processes (Wang et al., 2018). Primary productivity and the upwelling of the subsurface Kuroshio Current (KC) are the primary processes that contribute to dissolved oxygen in the East China Sea (ECS) (Gallagher et al., 2009, 2015). The decomposition of organic matter below the surface consumes dissolved oxygen, reducing the amount of dissolved oxygen in deep oceanic water (Joos et al., 2003). Productivity in the upper layer is linked to the nutrient arrival associated with the East Asian Summer Monsoon (EASM) in the ECS (Hu & Wang, 2016; Watanabe et al., 2007). The influx of terrestrial organic matter in the ECS is regulated by active river discharge and run-off associated with seasonal EASM precipitation variability (Lee et al., 2001; Matsuzaki et al., 2016). It is likely that the influence of EASM driven productivity and upwelling of the subsurface KC also varied on glacial-interglacial and shorter time scales. The residence time of oxygen in the deep-water is

often around thousands of years (Wang et al., 2018; Yamamoto et al., 2015), whereas the removal of subsurface oxygenated water depends upon the consumption of dissolved oxygen by sinking organic matter (Levin, 2002). The amount of dissolved oxygen is also dependent on the transport of oxygen-rich deep-water, biological productivity, and the amount and rate of burial of carbon-rich organic matter. Temperature and salinity are other factors, which determine the solubility of oxygen in oceanic water (Joos et al., 2003).

Various proxies have been used to assess the variability of deep-water oxygenation. Some of these proxies are benthic foraminiferal oxygen index (BFOI) (Kaiho, 1994, 1999; Kaminski, 2012; Wang et al., 2018), Mo/Al (Wang et al., 2018), I/Ca (Taylor et al., 2017), the number of pores in epifaunal benthic foraminifera (Rathburn et al., 2018), the grey color reflectance index (L*) (Huang et al., 2019; Irino et al., 2018; Kido et al., 2007; Tada et al., 1999; Watanabe et al., 2007), etc. Recently, Matsuzaki et al., (2019) characterized deep-water oxygenation in the ECS using the relative abundance of the radiolarian species *Cycladophora davisiana* from IODP Site U1429. These authors suggested that *C. davisiana*, which inhabits water depths below 500 m and is typically an oxic species, is a good indicator of deep-water oxygenation. However, as a planktic species this taxon cannot be used to estimate oxygenation at the sediment-water interface, nor to monitor the variability in suboxic to dysoxic conditions during climate transition phases. Furthermore, the relative abundance of *C. davisiana* is very low (~ 5%) between MIS 11 and MIS 6 and rare in strata younger than MIS 6 (Matsuzaki et al., 2019).

Benthic foraminifera inhabit the seafloor near the sediment-water interface, and are useful proxies to assess bottom water oxygenation (e.g., Burkett et al., 2016; Moumita Das et al., 2017; Lutze & Thiel, 1989; Rathburn et al., 2018). Surface productivity and the associated organic matter flux to the seafloor as well as dissolved oxygen in bottom water are major factors controlling the distribution of particular species of benthic foraminifera (Moumita Das et al., 2017; Fontanier et al., 2002; Jorissen et al., 2007; Sen Gupta & Machain-Castillo, 1993; Y. Zhou et al., 2016). The population abundance, diversity, chemical composition of tests, assemblage, size, and habitat (epifaunal, shallow infaunal and deep infaunal) of benthic foraminifera vary with bottom water conditions (Barik et al., 2019; Rathburn et al., 2018). Jorissen et al. (2007) suggested that faunal diversity and density are generally influenced by bottom water oxygenation and sediment pore water oxygenation. Therefore, benthic foraminifera provide ideal proxies to retrace the evolution of bottom water oxygenation and organic export flux to the sea floor through time.

This study reconstructs shifts in bottom water oxygenation along with variability in organic export flux in the ECS over the last 400 kyr using benthic foraminiferal assemblages from the Integrated Ocean Drilling Program (IODP) Site U1429. Multivariate analysis and environmental preferences of benthic foraminifera are used in addition to total organic carbon (TOC wt. %) and $CaCO_3$ (%) data (Black et al., 2018), the radiolarian species *Cycladophora davisiana* abundance (%) (Matsuzaki et al., 2019), $\delta^{13}C_{pf}$ and $\delta^{18}O_{bf}$ (Clemens et al., 2018) from the same site.

2 Site Location and Oceanographic Setting

Integrated Ocean Drilling Program Site U1429 (31°37.04'N, 128°59.85'E) (Fig. 1) in the ECS was cored down to 182 meters below sea floor (mbsf) at a water depth of 732 meters below sea level (mbsl; Tada et al., 2015). This site is located in the Danjo Basin on the western continental slope of the northern Okinawa Trough in the northeastern ECS (Fig. 1). The sediment succession at this site is mainly composed of calcareous nannofossil ooze and calcareous nannofossil-rich clay (Tada et al., 2015; D. Zhao et al., 2019). The KC and the Taiwan Warm Current (TWC) strongly influence the surface and subsurface waters of the ECS (e.g., Matsuzaki et al., 2016). The KC brings oxygen-rich, warm, saline and oligotrophic water to the ECS from the north equatorial Pacific region (Gallagher et al., 2015; Lee et al., 2001; Matsuzaki et al., 2019, 2016; Vats et al., 2020), while subsurface KC-driven upwelling (Chen et al., 1995; Liu et al., 1992; Vats et al., 2020; Wu et al., 2008; P. Zhou et al., 2018) brings nutrients and influences primary productivity. The other major component in the ECS is Changjiang Diluted Water (CDW), which brings freshwater from northwestern China and lowers the salinity and temperature in the ECS (Ichikawa & Beardsley, 2002). The CDW is associated with EASM precipitation, and its influence is seasonal (Lee et al., 2001; Matsuzaki et al., 2016). The CDW discharge also brings nutrients affecting biological productivity and the accumulation of terrestrial organic matter in the ECS. The sinking of organic matter to the bottom of the ECS consumes the available bottom water dissolved oxygen. Hence, enhanced subsurface KC upwelling and stronger EASM strongly influenced the bottom water oxygenation in the ECS. The modern annual (2013) dissolved oxygen concentration at the sediment-water interface near to the studied site is ~1.6 ml/l (Fig. S1; Garcia et al., 2013). The

decadal average (1955-2017) bottom water salinity and temperature at sediment-water interface is ~34.35 (Fig. S1; Zweng et al., 2019) and ~4°C (Fig. S1; Locarnini et al., 2019) respectively.

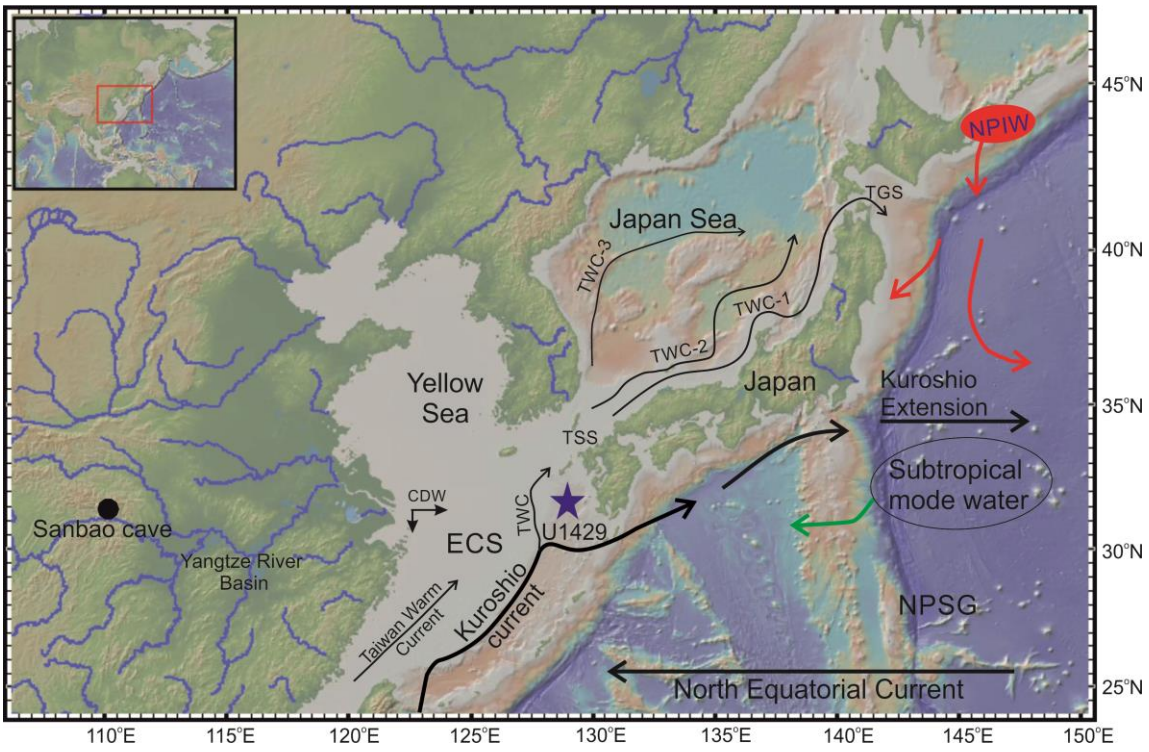

Figure 1. Location of IODP Site U1429 (31°37.04'N, 128°59.85'E, 732 mbsl) in the East China Sea (Blue star). Location of the Sanbao cave in China (Filled black circle). Black arrows indicate surface current directions. CDW– Changjiang Diluted Water, NPIW– North Pacific Intermediate Water, TWC– Tsushima Warm Current, NPSG– North Pacific Subtropical Gyre, TSS– Tsushima Strait, TGS– Tsugaru Strait. Surface currents marked after D. Zhao et al., (2017). This map was made with GeoMapApp (http://www.geomapapp.org) using the GMRT data set (Ryan et al., 2009).

3 Materials and Methods

A total of 225 sediment core samples (of 10 cc volume) were analyzed from IODP Site U1429, down to 182 mbsf. We used the high-resolution age model published by Clemens et al. (2018), which shows that the sediment succession extends back to ~400 ka. The upper part of the succession (back to 40 ka) was further constrained by 16 AMS ^{14}C dates (Vats et al., 2020; D. Zhao et al., 2017). The average temporal resolution per sample is ~2 kyr (Vats et al., 2020). The same

age model was also used to plot TOC (%), $CaCO_3$ (%) (Black et al., 2018), $\delta^{13}C_{pf}$ and $\delta^{18}O_{bf}$ (Clemens et al., 2018) and the *Cycladophora davisiana* (%) abundance data (Matsuzaki et al., 2019). Out of 225 samples, 36 samples yielded fewer than 30 specimens of foraminifera per 10 cc sediment, and these samples were discarded from the statistical analysis, as they may lead to artefacts. Most of these discarded samples are from the tephra layers within the core (Sagawa et al., 2018; Tada et al., 2015).

The samples were processed and analyzed following the standard methods outlined by Manisha Das et al. (2018). Benthic foraminiferal census data were generated for each sample from the >125 µm size fraction, and species abundance (percentage) was calculated. Benthic foraminiferal classification follows Loeblich and Tappan (1988) at the genus level and follows Manisha Das et al. (2021, 2018), Gallagher et al. (2018), Holbourn et al. (2013), Scott et al. (2000), and Zwaan et al. (1986) at the species level. Two hundred thirty-nine species of benthic foraminifera belonging to 96 genera were identified.

Of the 239 species identified, only 32 species (Fig. 2) with an abundance of ≧5% in 5 or more samples were selected for multivariate analysis. Exploratory factor analysis was performed on these species and to maximize the variance “fa” function and “pa” method (principal axes) of Psych package (Revelle, 2019; RStudio Team, 2020) were used. Based on scree-plot (X-Y) of eigenvalues, five factors were retained. Hierarchal cluster analysis was performed using Ward’s minimum linkage method for the same 32 species, which enabled to retain 6 clusters (Manisha Das et al., 2021; RStudio Team, 2020; Fig. S2). Incorporating consistent results from exploratory factor analysis and hierarchal cluster analysis, six biofacies of benthic foraminifera were identified in the ECS (Table 1). Each biofacies was named after the most dominant species with the highest factor loadings within each factor association. Biofacies abundance (%) was calculated based on cumulative percentages of all species contributing to that particular biofacies (Fig. 3). We have further classified and grouped these dominant 32 species into oxic, suboxic, and dysoxic species based on their environmental (oxygenation) preferences (Table 2).

152 Table 1. Benthic Foraminiferal Biofacies, Factor Scores and their preferred environments
153 at Site U1429.

Biofacies	**Factor Scores**	**Environment**	**Age (ka)**
1. **Biofacies Gv (**Factor 1^{-ve})		High energy conditions, pulsed food supply, oxic to slightly suboxic bottom water conditions	23-14
Gavelinopsis sp.	-0.64		
Oridorsalis umbonatus	-0.49		
Gyrodinoides cibaoensis	-0.46		
Quinqueloculina seminulum	-0.36		
2. **Biofacies Co** (Factor 2^{+ve})		High productivity, high food supply, highly dysoxic bottom water conditions	206, 93-41, and 27-17
Chilostomella oolina	0.81		
Fursenkoina rotundata	0.52		
Globobulimina pacifica	0.36		
3. **Biofacies Hb** (Factor 4^{-ve})		Moderate to high influx of organic Carbon, suboxic bottom water conditions	302-295, 39-30, and 15-0
Hyalinea balthica	-0.46		
Bulimina mexicana	-0.44		
Hoeglundina elegans	-0.36		
Valvulineria sadonica	-0.32		
4. **Biofacies Ct** (Factor 3^{+ve})		Enhanced but pulsed flux of phytodetritus, suboxic conditions with intermittent dysoxic conditions	331, 278-262, 153, 114-107, and 60-57
Cassidulina teretis	0.74		
Epistominella exigua	0.53		
Cassidulina laevigata	0.47		
Bolivina robusata	0.47		
Globocassidulina subglobosa	0.42		
5. **Biofacies Um** (Factor 5^{-ve})		High productivity, high influx of organic matter, suboxic to slightly dysoxic bottom water conditions	390-386, 282-218, 188-138, and 29-1
Uvigerina mediterranea	-0.55		
Uvigerina pygmea	-0.49		
Uvigerina peregrina	-0.47		
6. **Biofacies Mc** (Factor 1^{+ve})		Suboxic bottom water conditions, high organic carbon flux	396-283, 248-242, 212-193, 158, 135-122, 74 and 61
Martinotiella communis	0.44		
Gaudryina sp.	0.41		
Amphicoryna scalaris	0.33		
Uvigerina auberiana	0.33		
Melonis barleeanum	0.32		
Bulimina aculeata	0.32		

154

155 Table 2. List of oxic, suboxic, and dysoxic species recorded at Site U1429.

Type:	Microhabitat	Species:
Oxic Species	Epifaunal	*Cibicidoides mundulus* (Kaiho, 1994; Pérez-Asensio et al., 2017)
	Epifaunal	*Cibicidoides wuellerstorfi* (Moumita Das et al., 2017; De & Gupta, 2010; Kaiho, 1994)
	Epifaunal	*Epistominella exigua* (Bhaumik et al., 2007; De & Gupta, 2010)
	Epifaunal	*Gavelinopsis sp.* (Akimoto & Hasegawa, 1989; Takata et al., 2018)
	Epifaunal	*Globocassidulina subglobosa* (Araújo et al., 2018; Kaiho, 1994; Kaminski, 2012; Verma et al., 2013)
	Epifaunal	*Quinqueloculina seminulum* (Moumita Das et al., 2017; Hayward et al., 1997; Kaminski, 2012; Laprida et al., 2007)
	Epifaunal	*Sigmoilopsis schlumbergeri* (Kaminski, 2012; Mackensen et al., 1995; Saravanan et al., 2019)
Suboxic Species	Shallow infaunal	*Amphicoryna scalaris* (García-Sanz et al., 2018; Kaminski, 2012)
	Intermediate to deep infaunal	*Bulimina aculeata* (Moumita Das et al., 2017; Kaiho, 1994; Kaminski, 2012)
	Deep infaunal	*Bulimina marginata* (Moumita Das et al., 2017; Kaminski, 2012; Saravanan et al., 2019)
	Infaunal	*Bulimina mexicana* (Grunert et al., 2018)
	Shallow infaunal	*Cassidulina laevigata* (Bubenshchikova et al., 2010; Schmiedl et al., 1997)
	Infaunal	*Cassidulina teretis* (Cronin et al., 2019; Mackensen & Hald, 1988)
	Shallow to deep infaunal	*Gaudryina sp.* (Rostami et al., 2020)
	Epifaunal	*Gyroidinoides cibaoensis* (Bhaumik et al., 2007; Moumita Das et al., 2017; De & Gupta, 2010)
	Epifaunal	*Hoeglundina elegans* (Gupta & Thomas, 1999; Kaiho, 1994, 1999; Sarkar & Gupta, 2014)
	Shallow infaunal	*Hyalinea balthica* (Charrieau et al., 2018; Moumita Das et al., 2017; Kaminski, 2012)
	Intermediate infaunal	*Melonis barleeanum* (Fontanier et al., 2002, 2005; Kaminski, 2012; Schmiedl et al., 2000)
	Infaunal	*Martinottiella communis* (Culver & Buzas, 1987; Jian et al., 1999; Kender & Kaminski, 2017)
	Infaunal	*Nonionina communis* (Diz & Francés, 2008; Fontanier et al., 2002)
	Shallow infaunal to epifaunal	*Oridorsalis umbonatus* (Bubenshchikova et al., 2010; Moumita Das et al., 2017)
	Infaunal	*Pullenia bulloides* (Moumita Das et al., 2017; Gupta & Thomas, 1999; Rathburn & Corliss, 1994)
	Infaunal	*Pullenia quinqueloba* (Moumita Das et al., 2017; Kaminski, 2012; Wang et al., 2018)
	Shallow infaunal	*Uvigerina auberiana* (Bubenshchikova et al., 2010; Gorbarenko et al., 2004; Kuhnt et al., 1999; Schmiedl et al., 1997)
	Shallow infaunal	*Uvigerina mediterranea* (Manisha Das et al., 2018; Schmiedl et al., 2000)
	Shallow infaunal	*Uvigerina peregrina* (Manisha Das et al., 2018; Lutze, 1979; Schmiedl et al., 1997; Schmiedl & Leuschner, 2005)
	Shallow infaunal	*Uvigerina pygmaea* (Manisha Das et al., 2018; Kastens & Mascle, 1990; Lutze, 1979)
	Intermediate infaunal	*Valvulineria sadonica* (Bubenshchikova et al., 2010)
Dysoxic Species	Infaunal	*Bolivina robusta* (Haller et al., 2018; Kaiho, 1994; B. Zhao et al., 2018)
	Deep infaunal	*Chilostomella oolina* (Kaiho, 1994; McGann & Conrad, 2018; Wang et al., 2018)
	Infaunal	*Fursenkoina rotundata* (Moumita Das et al., 2017; Kaiho, 1994; Patarroyo & Martínez, 2015)
	Deep infaunal	*Globobulimina pacifica* (Moumita Das et al., 2017; McGann & Conrad, 2018)

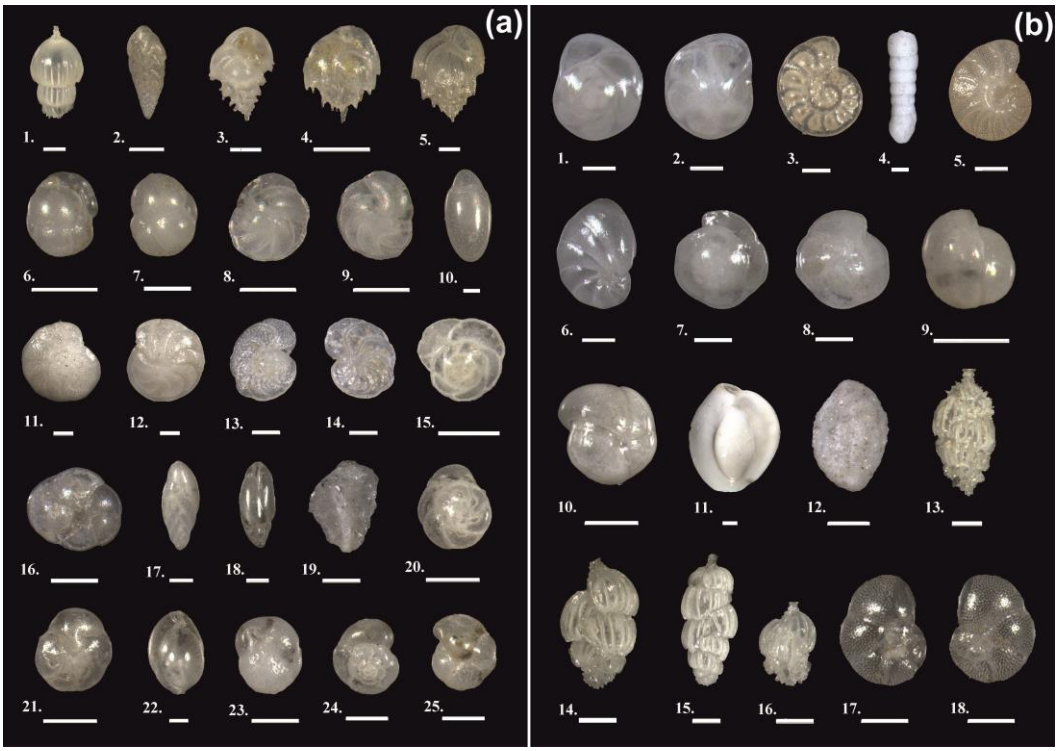

Figure 2. Microphotographs of the dominant benthic foraminifera (32 species) present at Site U1429. Plate (a): 1. *Amphicoryna scalaris* (side view) 2. *Bolivina robusta* (side view) 3. *Bulimina aculeata* (side view) 4. *Bulimina marginata* (side view) 5. *Bulimina mexicana* (side view) 6. *Cassidulina laevigata* (umbilical view) 7. *Cassidulina laevigata* (spiral view) 8. *Cassidulina teretis* (umbilical view) 9. *Cassidulina teretis* (spiral view) 10. *Chilostomella oolina* (side view) 11. *Cibicidoides mundulus* (spiral view) 12. *Cibicidoides mundulus* (umbilical view) 13. *Cibicidoides wuellestorfi* (spiral view) 14. *Cibicidoides wuellestorfi* (umbilical view) 15. *Epistominella exigua* (spiral view) 16. *Epistominella exigua* (umbilical view) 17. *Fursenkoina rotundata* (side view) 18. *Fursenkoina rotundata* (apertural view) 19. *Gaudryina* sp. (side view) 20. *Gavelinopsis* sp. (spiral view) 21. *Gavelinopsis* sp. (umbilical view) 22. *Globobulimina pacifica* (side view) 23. *Globocassidulina subglobosa* (apertural view) 24. *Gyroidinoides cibaoensis* (spiral view) 25. *Gyroidinoides cibaoensis* (umbilical view); Plate (b): 1. *Hoeglundina elegans* (spiral view) 2. *Hoeglundina elegans* (umbilical view) 3. *Hyalinea balthica* (spiral view) 4. *Martinottiella communis* (side view) 5. *Melonis barleenaum* (spiral view) 6. *Nonionina communis* (side view) 7. *Oridorsalis umbonatus* (spiral view) 8. *Oridorsalis umbonatus* (umbilical view) 9. *Pullenia bulloides* (side view) 10. *Pullenia quinqueloba* (side view) 11. *Quinqueloculina seminulum* (side view) 12. *Sigmoilopsis schlumbergeri* (side view) 13. *Uvigerina auberiana* (side

174 view) 14. *Uvigerina mediterranea* (side view) 15. *Uvigerina peregrina* (side view) 16. *Uvigerina*
175 *pygmaea* (side view) 18. *Valvulineria sadonica* (umbilical view) 19. *Valvulineria sadonica* (spiral
176 view) [All Scale bars = 100 μm].

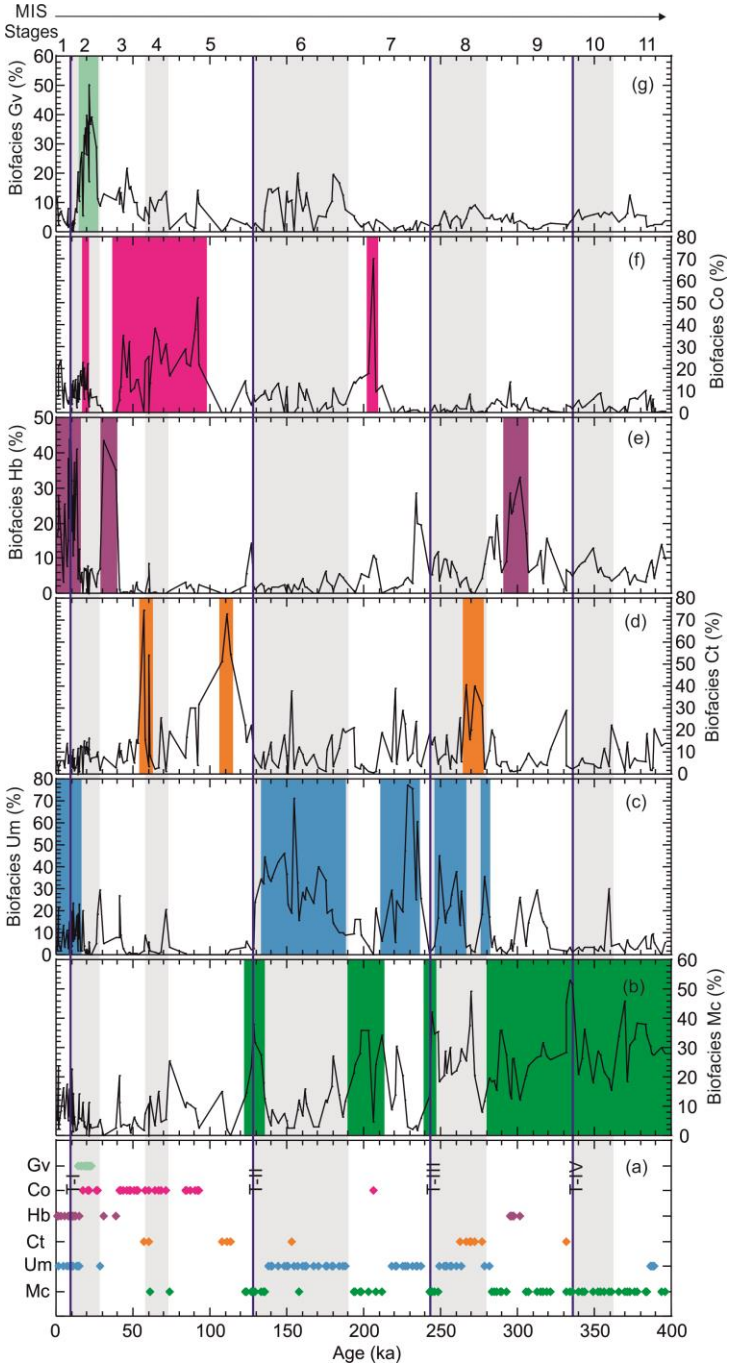

177

178 Figure 3. Benthic foraminiferal biofacies at Site U1429 plotted against interpolated ages (a-g), (a,
179 b) Green shading and diamond indicate biofacies Mc (%), (a, c) Blue shading and diamond indicate
180 biofacies Um (%), (a, d) Orange shading and diamond indicate biofacies Ct (%), (a, e) Purple

shading and diamond indicate biofacies Hb (%), (a, f) Pink shading and diamond indicate biofacies Co (%), (a, g) Light green shading and diamond indicate biofacies Gv (%). Mc- *Martinottiella communis*, Um- *Uvigerina mediterranea*, Ct- *Cassidulinia teretis*, Hb- *Hyalinea balthica*, Co- *Chilostomella oolina*, Gv- *Gavelinopsis* sp. Dark grey bars indicate MIS stages. Dark blue lines mark the termination events T-I, T-II, T-III, and T-IV.

The diversity among benthic foraminifera was calculated using the Shannon Index (H) (Shannon & Weaver, 1949), given by the formula:

$$H = -\sum_{i=1}^{S} \boldsymbol{p_i \, ln \, p_i} \quad (1)$$

where, S is the number of species in a given sample, p_i is the proportion of the i^{th} species in the sample, and ln is the natural logarithm.

Spectral analysis was carried out using PAST 4.03 program (Hammer et al., 2001) for the oxic genus *Quinqueloculina* (%), suboxic genus *Bulimina* (%), and dysoxic genus *Globobulimina* (%) and the productivity indicator $\delta^{13}C_{pf}$ (Clemens et al., 2018) over the investigated interval. We selected 'Welch' window parameter to obtain the spectra at a 90 % confidence level. The spectrum was bias-corrected using the Monte Carlo simulation option (Schulz & Mudelsee, 2002).

4 Results

4.1 Temporal variability of oxic, suboxic and dysoxic species in the ECS

Following previous approaches, we use the term dysoxic, when dissolved oxygen (DO) is 0.1–0.3 mL/L, suboxic, when DO is 0.3–1.5 mL/L, and oxic, when DO is >1.5 mL/L (e.g., Gallagher et al., 2018; Kaiho, 1994; Wang et al., 2018). At Site U1429, most of the oxic species are epifaunal, the suboxic species are shallow to deep infaunal, and the dysoxic species are deep infaunal (Table 2). Since MIS 11 (~400 ka), oxic species were relatively less abundant in the ECS and did not show any significant variations in trends except for a peak just after T-III followed by intermittent occurrences during MIS 1 (Fig. 4). The temporal variability of the dominant oxic genus *Quinqueloculina* followed a relatively similar trend (Fig. S3). Suboxic species were abundant between MIS 11 and 6, subsequently decreased during MIS 5 and 4, and increased once more in abundance between MIS 3 and 1 (Fig. 4). The temporal variation of the suboxic genus

Bulimina exhibits an overall similar trend, but displays higher variability (Fig. S3). Dysoxic species were relatively abundant during MIS 7 and 5, but abundance decreased between MIS 5 and 4, and they became relatively rare between MIS 3 and 2 (Fig. 4). The dysoxic genus *Globobulimina* generally follows the same trend, but shows higher abundance during MIS 5 (Fig. S3).

4.2 Biofacies analysis

For the identified six biofacies *Gavelinopsis* sp. (Gv), *Chilostomella oolina* (Co), *Hyalinea balthica* (Hb), *Cassidulinia teretis* (Ct), *Uvigerina mediterranea* (Um), and *Martinottiella communis* (Mc) (Table 1), environmental significance is inferred, based on environmental preferences of individual species of that particular biofacies.

4.2.1 Biofacies Gv

The biofacies Gv has high negative factor loading in Factor 1 and includes four species: *Gavelinopsis* sp., *Oridorsalis umbonatus*, *Gyroidinoides cibaoensis*, and *Quinqueloculina seminulum* (Table 1). This biofacies occurs almost continuously in 13 samples between 23 and 14 ka (Fig. 3). *Gavelinopsis* sp. is an epifaunal species found in the inner sublittoral zone of the Japanese coast (Akimoto & Hasegawa, 1989; Takata et al., 2018) and often inhabits high energy environments affected by the wave and current processes (Takata et al., 2018). *Oridorsalis umbonatus* is a cosmopolitan species present over a range of water depths and trophic levels (Gupta et al., 2006; Schmiedl & Mackensen, 1997; Takata et al., 2019). It has also been reported as a suboxic and shallow infaunal to epifaunal species (Bubenshchikova et al., 2010; Jorissen et al., 1998). *Gyroidinoides cibaoensis* is found in a wider range of oxygen conditions with variable food availability (De & Gupta, 2010). *Quinqueloculina seminulum* is a cold-water dweller (Hayward et al., 1997), found in high-energy conditions (Laprida et al., 2007) with a pulsed food supply (Gupta & Thomas, 2003; Sarkar & Gupta, 2014; Takata et al., 2018), generally in shallow marine environments (Murray, 2006). Biofacies Gv overall indicates relatively high energy, inner to outer

shelf environment with a pulsed food supply and overall oxic to slightly suboxic bottom water conditions.

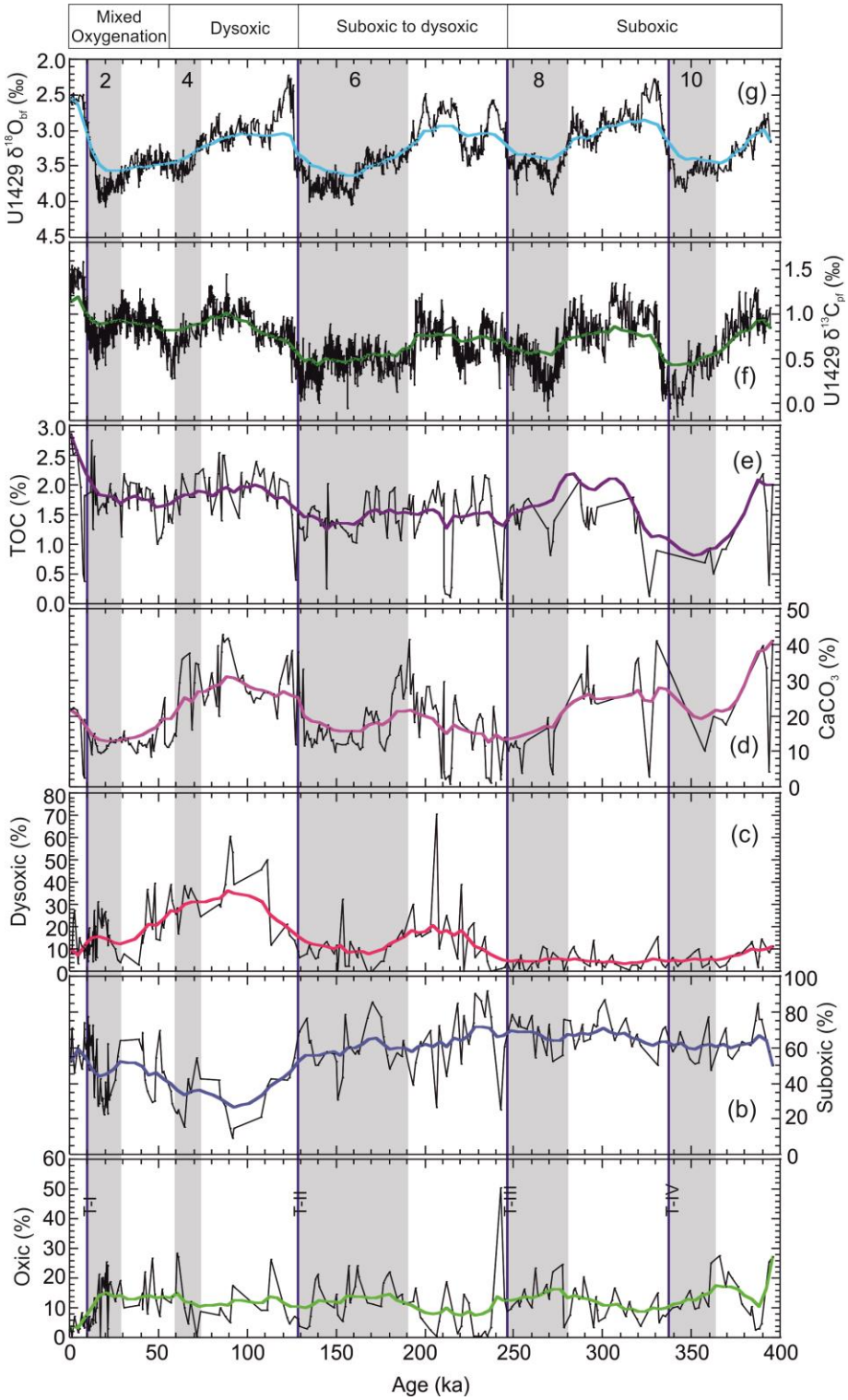

Figure 4. Plot of (a) Oxic species abundance (%), (b) Suboxic species abundance (%), (c) Dysoxic species abundance (%), (d) CaCO3 (%) and (e) TOC (%) (Black et al., 2018); (f) δ13Cpf (‰) and

(g) Benthic foraminiferal $\delta^{18}O_{bf}$ (Clemens et al., 2018) plotted against age at Site U1429. Dark blue lines mark the termination events T-I, T-II, T-III, and T-IV. The colored bold curves are smooth curve fit applied using KaleidaGraph software (Manisha Das et al., 2021). Dark grey bars indicate MIS stages.

4.2.2 Biofacies Co

Biofacies Co is defined by the species having high positive factor loadings on Factor 2 (Table 1). *Chilostomella oolina*, *Fursenkoina rotundata*, and *Globobulimina pacifica* are characteristic species of this biofacies. This biofacies occurs in 29 samples, almost continuously between ~93 and 41 ka and occasionally at other times (Fig. 3). *Chilostomella oolina* is a deep infaunal species typifying dysoxic conditions (Jorissen et al., 1998; McGann & Conrad, 2018) with high productivity (Wang et al., 2018). *Fursenkoina rotundata* is an infaunal, dysoxic, opportunist species (Moumita Das et al., 2017), present in areas where there is significant organic matter influx associated with high surface productivity leading to low-oxygen conditions (Patarroyo & Martínez, 2015). *Globobulimina pacifica* is also a low oxygen tolerant taxon (Ballesteros-Prada, 2019; Bernhard et al., 1997; McGann & Conrad, 2018). It occupies intermediate to deep-infaunal microhabitats in dysoxic conditions (Moumita Das et al., 2017) and is commonly associated with poorly ventilated deep-water (Ma et al., 2019). Biofacies Co indicates strongly dysoxic bottom water conditions in the ECS associated with high productivity.

4.2.3 Biofacies Hb

Biofacies Hb has high negative factor loadings on Factor 4 (Table 1). *Hyalinea balthica*, *Bulimina mexicana*, *Hoeglundina elegans*, and *Valvulineria sadonica* are characteristic species of this biofacies. This biofacies is present in 22 samples at ~302-295, ~39-30 and ~15-0 ka (Fig. 3). *Hyalinea balthica* is a shallow infaunal, opportunistic species present in food-abundant regions and suboxic conditions (Charrieau et al., 2018; Moumita Das et al., 2017). *Bulimina mexicana* is a cosmopolitan taxon that thrives in the intermediate (bathyal) water depths in all ocean basins (Culver & Buzas, 1980; Grunert et al., 2018; Jones & Brady, 1994; Van Morkhoven et al., 1986). It generally prefers shallow infaunal microhabitat, high fluxes of organic matter and oxygen-depleted sediments (Grunert et al., 2018). *Hoeglundina elegans* is a shallow infaunal taxon (Gonzales et al., 2017; Jorissen et al., 1998) and was reported in the upwelling zones of the Bay

of Biscay (Martínez-García et al., 2013). The species is present in moderately oxygen-depleted environments in the Arabian Sea and is considered as suboxic species (Gupta & Thomas, 1999; Kaiho, 1994, 1999; Sarkar & Gupta, 2014). *Valvulineria sadonica* is found in areas with a high flux of degraded and refractory organic matter in shallow subsurface water (Gorbarenko et al., 2010; Phleger & Soutar, 1973; Smith, 1964). It is an intermediate infaunal species typifying mostly suboxic conditions and within the OMZ (Oxygen Minimum Zone) in the Okhotsk Sea (Bubenshchikova et al., 2010). Biofacies Hb suggests a high influx of organic matter and overall suboxic bottom water conditions.

4.2.4 Biofacies Ct

Biofacies Ct is characterized by five species *Cassidulina teretis*, *Epistominella exigua*, *Cassidulina laevigata*, *Bolivina robusta*, and *Globocassidulina subglobosa* with positive high factor loadings on Factor 3 (Table 1). This biofacies occurs sporadically in 13 samples at 331, 278-262, ~153, 114-107, ~60 and ~57 ka (Fig. 3). *Cassidulina teretis* is a common high latitude species present in the cold Arctic Ocean and off Alaska (Cronin et al., 2019; Mackensen & Hald, 1988). This species typifies seasonally ice-free regions and is associated with high productivity and high phytodetritus influx (Cronin et al., 2019; Scott et al., 2008). *Epistominella exigua* is a cosmopolitan species feeding opportunistically on phytodetritus deposited seasonally on the seafloor and can tolerate a varying organic export flux (Manisha Das et al., 2021; Gooday, 1988; R. K. Singh & Gupta, 2004, 2010). *Cassidulina laevigata*, is a shallow infaunal taxon (Fontanier et al., 2002), typifying relatively cold waters with high organic matter content (Pascual et al., 2020), and is tolerant of moderate oxygen depletion in bottom and pore water under high organic flux rates (Manisha Das et al., 2021; Nardelli et al., 2014; Sen Gupta & Machain-Castillo, 1993). *Bolivina robusta* is an open ocean infaunal species found in temperate to subtropical middle to upper bathyal depths (Haller et al., 2018; B. Zhao et al., 2018). *Bolivina robusta* may be able to tolerate high eutrophication and is a useful indicator of low oxygen condition at the seafloor (B. Zhao et al., 2018). *Globocassidulina subglobosa*, which prefers oxic conditions and high to intermediate food supply, is a cosmopolitan epifaunal species (Araújo et al., 2018; Manisha Das et al., 2021; Kaminski, 2012; Martins et al., 2007; Murray, 2006; Verma et al., 2013). Biofacies Ct indicates

an enhanced phytodetritus flux into the ECS associated with suboxic conditions that occasionally become dysoxic, as shown by the presence of *B. robusata*.

4.2.5 Biofacies Um

Biofacies Um has high negative factor loadings on Factor 5 (Table 1). It is comprised of *Uvigerina mediterranea*, *Uvigerina pygmea*, and *Uvigerina peregrina*. This biofacies is present in 55 samples at ~390-386, ~282-218, 188-138, and ~29-1 ka (Fig. 3). *Uvigerina mediterranea* is a low to intermediate oxygen tolerant shallow infaunal species of middle to lower bathyal depths (Manisha Das et al., 2018, 2021; Duros et al., 2011; Schmiedl et al., 2000; Schweizer, 2006; A. D. Singh et al., 2015). *Uvigerina pygmea* is also a shallow infaunal species, typical of intermediate to low oxygen environments in deep-water masses (Kastens & Mascle, 1990; Lutze, 1979). The environmental preferences of *Uvigerina pygmea* are similar to that of *Uvigerina peregrina* (Manisha Das et al., 2018). *Uvigerina peregrina* is a shallow infaunal species (Jorissen et al., 1998) typical of middle neritic to lower bathyal depths (Schweizer, 2006). It is often associated with high productivity and sustained flux of organic matter and can tolerate lower food levels and oxygen deficiency (Manisha Das et al., 2018, 2021; Moumita Das et al., 2017; Gupta et al., 2008; Mazumder & Nigam, 2014). Biofacies Um suggests suboxic to dysoxic bottom water conditions in the ECS with a relatively higher influx of organic matter.

4.2.6 Biofacies Mc

Biofacies Mc has high positive factor loadings in Factor 1 (Table 1) and is characterized by two agglutinated species: *Martinottiella communis* and *Gaudryina* sp. along with the calcareous species *Amphicoryna scalaris*, *Melonis barleeanum*, *Uvigerina auberiana*, and *Bulimina aculeata*. It is present in 57 samples at ~396-283, ~248-242, ~212-193, ~158, ~135-122, 74 and ~61 ka (Fig. 3). *Martinottiella communis* is an agglutinated foraminifer, often found in shelf to bathyal conditions (Kaiho & Nishimura, 1992), and maybe present in high organic carbon flux and tolerant to moderate to low oxygen settings (Kender & Kaminski, 2017) and found within DO range 4.7 to 5.7 mL/L in the Scotia Sea and Argentine Basin (Harloff & Mackensen, 1997). *Gaudryina* sp. is also an agglutinated species that has a shallow to deep infaunal habitat (Reolid et al., 2012). It has been reported as an endobenthic species associated with moderately oxygenated environments (Rostami et al., 2020). *Amphicoryna scalaris* is a shallow infaunal species (Balestra et al., 2017),

associated with high input of labile organic matter (Fontanier et al., 2008), and has been reported in moderately oxygenated environments (García-Sanz et al., 2018). The environmental preference of *Melonis barleeanum*, often associated with degraded refractory organic matter, is an infaunal species found in moderately oxygen-depleted condition (Fontanier et al., 2002, 2005; Schmiedl et al., 2000). The shallow infaunal *Uvigerina auberiana*, reported as a suboxic species the in Okhotsk Sea (Bubenshchikova et al., 2010; Gorbarenko et al., 2004), prefers a higher organic carbon flux and has also been reported in South China Sea (Kuhnt et al., 1999). *Bulimina aculeata* is an intermediate to deep infaunal taxon, mostly abundant in suboxic bottom water conditions (Moumita Das et al., 2017; Kaiho, 1994; Kaminski, 2012). Biofacies Mc suggests suboxic bottom water conditions in the ECS with high organic export flux.

4.3 Temporal variability of marine productivity indicators in the ECS

Marine productivity indicators such as $CaCO_3$ (%), TOC (%) (Black et al., 2018), and $\delta^{13}C_{pf}$ (‰) (Clemens et al., 2018) are used to complement the benthic foraminiferal distribution data. $CaCO_3$ (%) was relatively high (41.17 %) during mid-MIS 11, but gradually decreased to 10.13 % during MIS 10 (Fig. 4). $CaCO_3$ (%), increased again during MIS 9 with an average of 28.24 %, then decreased to its lowest value of 3.65 % during MIS 8 with an average value of 11.51 % during this interval. $CaCO_3$ (%) continued to be relatively low (average value 16.66 %) during MIS 7 and 6 (Fig. 4) before increasing to its highest value (42.84 %) during MIS 5 (average 29.76 %), then gradually decreased to modern-day values (21.54 %) after MIS 5 (Fig. 4). The TOC (%) trend at Site U1429 is comparable trend to that of $CaCO_3$ (%) between MIS 11 and MIS 8 with value between 2.2 % and 0.13 % (average 1.33 %), followed by small variations between 2.17 % and 0.77 % (average 1.39 %) until MIS 6 (Fig. 4). TOC (%) increased between MIS 5 and 1, and reached a maximum value of 2.85 % (Fig. 4). The $\delta^{13}C_{pf}$ (‰) values exhibit a decreasing trend toward MIS 10, ranging between 1.29 and 0.3 ‰ (VPDB), then gradually declined to -0.15 ‰ during MIS 10. During MIS 9, $\delta^{13}C_{pf}$ (‰) increased to 1.35 ‰, then declined to -0.08 ‰ during MIS 8. $\delta^{13}C_{pf}$ (‰) ranged between -0.06 ‰ and 1.22 ‰ during MIS 7 and MIS 6 with an average of 0.55 ‰ before increasing to 1.44 ‰ during MIS 5 and later declined during MIS 2. $\delta^{13}C_{pf}$ (‰)

increased to 1.58 ‰ during MIS 1. Overall, $\delta^{13}C_{pf}$ (‰) values exhibits a declining trend during all glacial intervals (MIS 2, 4, 6, 8 and 10) (Figs. 4, 5).

4.4 Spectral analysis

Spectral analysis of the oxic genus *Quinqueloculina* (%) shows prominent cyclicity of 106, 23, 7, and 6 kyr (Fig. 6a). The suboxic genus *Bulimina* (%) shows abundance peaks at 44, 23, 13, 11, 10, 5, and 4 kyr (Fig. 6b) and the dysoxic genus *Globobulimina* (%) at 132, 24, 8, 7, and 6 kyr (Fig. 6c). The spectral analysis of $\delta^{13}C_{pf}$ exhibits peaks at 105, 40, 28, 23 kyr (Fig. 6d).

5 Discussion

5.1 East China Sea bottom water oxygenation

5.1.1 MIS 11 to MIS 8

The ECS bottom water remained overall suboxic between MIS 11 and 8, as shown by the consistent occurrences of biofacies Mc, Ct and Hb (Fig. 3). The $\delta^{18}O_{bf}$ values from Site U1429 (Fig. 4) and composite $\delta^{18}O$ values from the Sanbao cave (Cheng et al., 2016; Clemens et al., 2018; Fig. 5) suggest that the EASM was relatively weak and productivity was low in the ECS during MIS 10 (Fig. 3). A weak monsoon likely reduced terrigenous organic matter flux leading to lower mass accumulation rates (lighter $\delta^{13}C_{pf}$; Clemens et al., 2018; Anderson et al., 2018) with relatively lower TOC (%) and $CaCO_3$ (%) (Black et al., 2018; Fig. 4). We suggest that the total amount of organic carbon sinking to the bottom of the ECS was minimal during MIS 10 and was associated with an oxic to suboxic water column, as indicated by the abundance of the oxic radiolarian species *C. davisiana* (Fig. 5; Matsuzaki et al., 2019) and the foraminiferal suboxic genus *Bulimina* and oxic genus *Quinqueloculina* (Fig. S3). During MIS 9, SST increased in the ECS and EASM precipitation became enhanced, leading to a higher CDW discharge (Vats et al., 2020) and to suboxic bottom water conditions that became dysoxic by the end of MIS 8 at termination T-III (biofacies Um; Figs. 3, 5). The prevalence of warm conditions is also supported by higher abundances of the shallow warm water radiolarian genus *Tetrapyle* (Matsuzaki et al., 2019) and the planktic foraminifera *Globigerinoides ruber* (Vats et al., 2020). Benthic foraminiferal diversity

(Shannon Index) was relatively constant between MIS 11 and 8 (Fig. 5), indicating that no major benthic foraminiferal turnover occurred during this phase of ECS bottom water evolution.

5.1.2 MIS 7 to MIS 6

Suboxic species shows a slight declining trend after MIS 8, while dysoxic species increase suggesting that bottom water became suboxic to dysoxic (Fig. 4). MIS 7 was characterized by generally low benthic foraminiferal diversity (H), relatively higher abundance of dysoxic species and dominance of the suboxic to dysoxic biofacies Um (Figs. 3, 4, 5). The ECS bottom water was overall suboxic to dysoxic during MIS 7, except for some transient low productivity events characterized by intermittent increases in suboxic biofacies Mc (Fig. 3). Nutrients transported by the CDW due to increased EASM precipitation increased primary productivity in shallow water (Matsuzaki et al., 2019) until MIS 6 (biofacies Um) and resulted in suboxic to slightly dysoxic bottom water conditions (Figs. 3, 4, 5). The KC was relatively weaker during MIS 6, suggested by the declining trend of KC indicator species *Globigerinodes ruber* (Vats et al., 2020), and SST varied within a range of ±1°C in the ECS (Clemens et al., 2018). However, the influx of the planktic foraminifera *Globorotalia inflata* indicates the onset of warmer conditions by the end of MIS 6 (Vats et al., 2020). The restriction of the KC during MIS 6, due to the associated low glacial sea-level, led to transient declines in benthic foraminiferal diversity (Fig. 5) and to changes in the relative abundance of dysoxic and suboxic species (Fig. 4).

5.1.3 MIS 5 to MIS 4

The beginning of MIS 5 was characterized by suboxic conditions with intermittent dysoxic episodes (biofacies Mc and Ct; Figs. 3, 5) between T-II and ~110 ka. The occurrence of biofacies Ct during MIS 5 indicates enhanced pulsed phytodetritus input in the ECS, which might be due to the strengthening of the KC and EASM. Nevertheless, dysoxic conditions prevailed from mid MIS 5 (~110 ka) to MIS 4, which is evident from the abundance of dysoxic species as well as *Globobulimina* genus and biofacies Co (Figs. 3, 5; Fig. S3). The T-II marks yet another major switch in bottom water oxygenation in the ECS, also accompanied by a substantial decrease in the oxic radiolarian species *C. davisiana*, suggesting depletion of dissolved oxygen within the water column. $CaCO_3$ (%), TOC (%), and $\delta^{13}C_{pf}$ (‰) values suggest higher productivity associated either with upwelling of the subsurface Kuroshio and/or increased influx from the CDW discharge (Vats

et al., 2020; Matsuzaki et al., 2019). The increased productivity and rapid sinking of organic matter may have utilized the dissolved oxygen from different levels of the water column, ultimately leading to dysoxic bottom water conditions in the ECS. The end of the glacial MIS 4 coincided with an improvement in bottom water oxygenation in the ECS, marked by the occurrence of biofacies Ct (Fig. 3). The marine productivity indicators and the dysoxic species exhibited declining trends, whereas the suboxic species displayed an increasing trend, which together suggests that productivity decreased by the end of MIS 4 (Fig. 4).

5.1.4 MIS 3 to MIS 1

Bottom water conditions in the ECS experienced variable oxygen concentrations between MIS 3 and 1, as shown by the variable occurrence of biofacies Um, Hb, Co and Gv (Figs. 3, 5). Despite a weaker KC during MIS 3 and 2, marine primary productivity remained high, suggesting a higher influx of terrigenous organic matter and nutrients delivered by the CDW due to an enhanced EASM (Vats et al., 2020). An increase in suboxic species abundance suggests the prevalence of suboxic as well as intermittent dysoxic conditions during MIS 3. The ECS water became oxic during the glacial MIS 2, as indicated by the occurrence of biofacies Gv and a slightly increasing trend of oxic species coincident with a declining trend of suboxic species (Figs. 3, 4, 5). During the last glacial maximum, sea level fell by ~120 m, and marine productivity declined significantly, promoting oxic bottom water conditions (Anderson et al., 2018; Kubota et al., 2010). Kubota et al. (2019) also suggested that the precipitation response of the EASM varied during MIS 3 and 2, which in turn may have influenced oxygen availability at the sea floor during termination event T-I. The alternations between biofacies Hb and Um and the shift from suboxic to oxic species (Figs. 3, 4, 5) during MIS 1 suggest variable bottom water oxygenation related to the variability of EASM precipitation and KC strength. However, higher-resolution studies are required to further constrain the variability of ECS deep-water oxygenation on a millennial to centennial-scale.

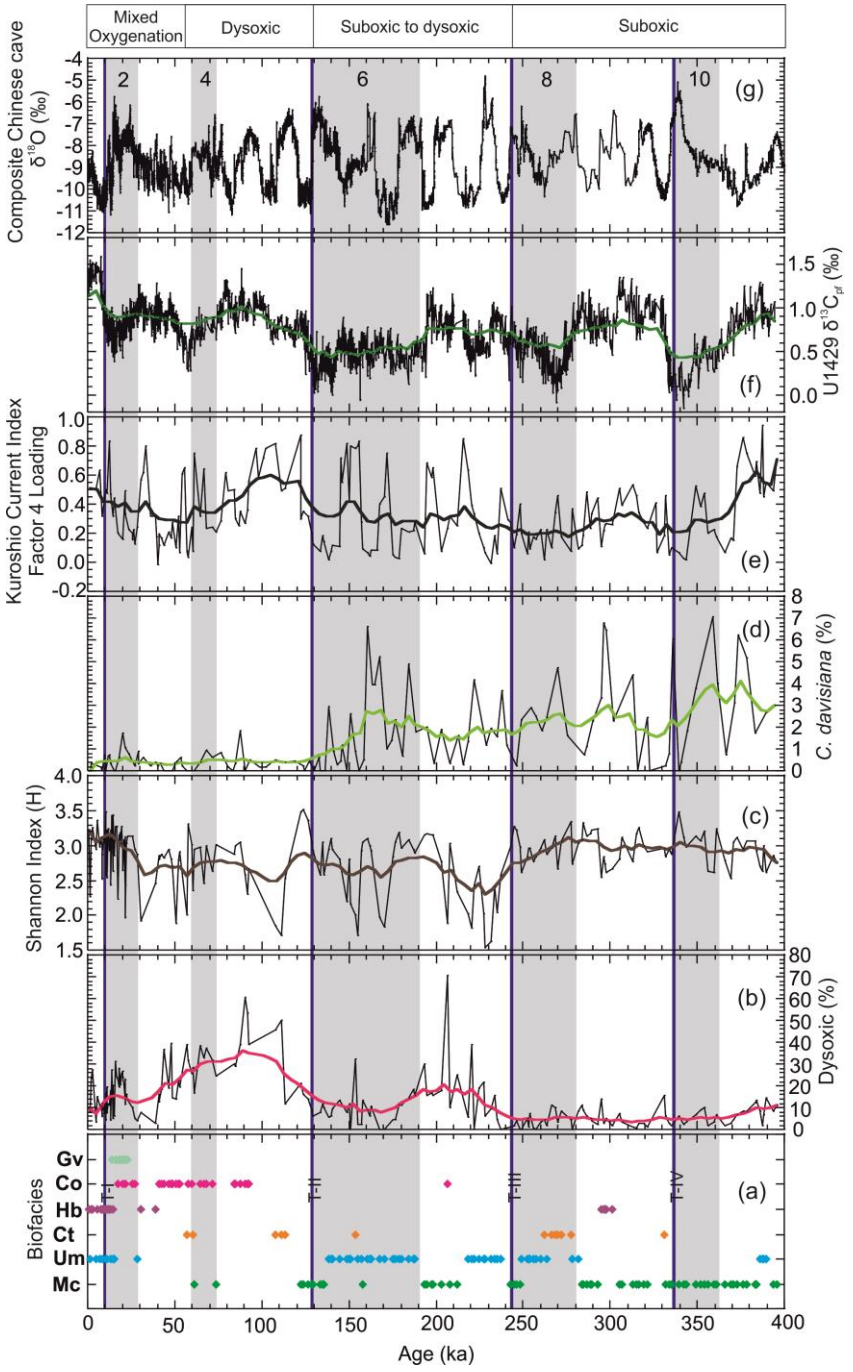

Figure 5. (a) Benthic foraminiferal biofacies, (b) Dysoxic species abundance (%), (c) Benthic foraminiferal diversity as Shannon Index (H) (d) Oxic radiolarian species *C. davisiana* (%) (Matsuzaki et al., 2019), (e) KC Index- Factor 4 loading (Vats et al., 2020), (f) $\delta^{13}C_{pf}$ (‰) (Clemens et al., 2018) at Site U1429, and (g) Asian Monsoon indicator- Composite Chinese cave $\delta^{18}O$ (‰) (Cheng et al., 2016). Dark blue lines mark termination events T-I, T-II, T-III, and T-IV. The

colored bold curves are smooth curve fit applied using KaleidaGraph software (Manisha Das et al., 2021). Dark grey bars indicate MIS stages.

5.2 Evolution of productivity and bottom water oxygenation in the ECS in relation to global climate trends

Benthic foraminiferal proxy data indicate marked variability in productivity, organic export flux and bottom water oxygenation over the last 400,000 years in the ECS. The oxic genus *Quinqueloculina* (%), and productivity indicators $\delta^{13}C_{pf}$ exhibits ~100 kyr cyclicity (Fig. 6). Clemens et al. (2018) suggest that glacial-interglacial climate variability exerted an important control on local seawater properties (i.e., riverine influx). Therefore, the oxygenation of ECS bottom water was likely influenced by EASM related primary productivity changes linked to variations in nutrient input derived from terrestrial organic matter in the ECS.

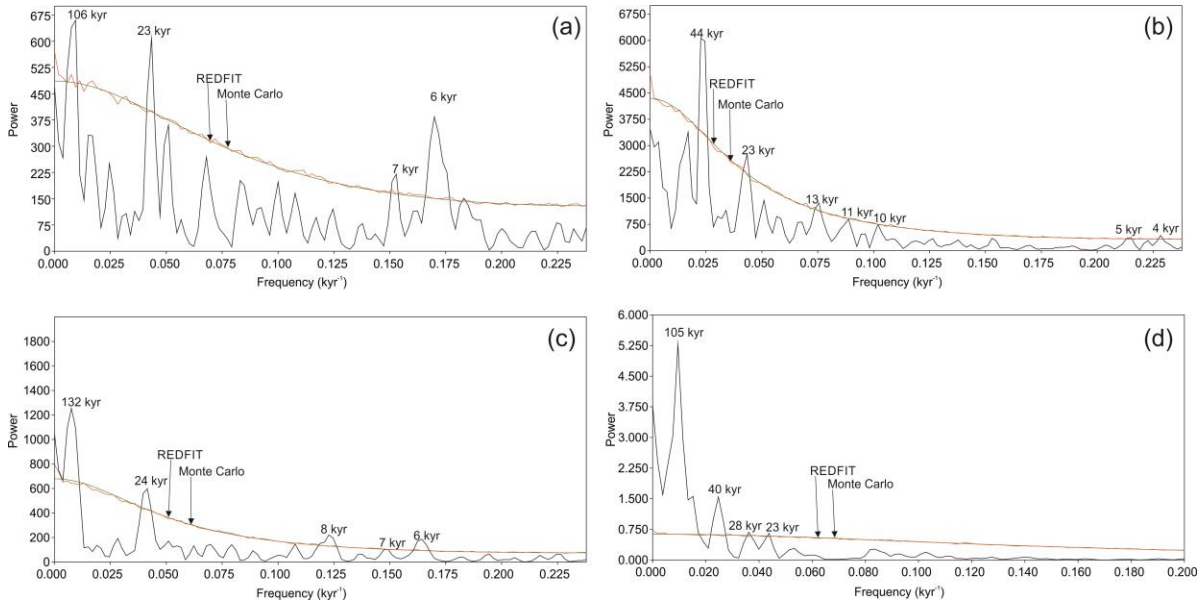

Figure 6. Spectral analysis of (a) oxic genus *Quinqueloculina* (%), (b) suboxic genus *Bulimina* (%), (c) dysoxic genus *Globobulimina* (%), and (d) $\delta^{13}C_{pf}$ (‰) at Site U1429 for the period 0 to 400 ka showing significant periodicities at 90% significance level.

Glacial-interglacial sea level changes additionally controlled the intensity of the KC intensity and the Tsushima warm current into the Japan Sea (Das et al., 2018, 2020; Gallagher et al., 2018; Saavedra-Pellitero et al., 2019). Spectral analysis of the oxic genus *Quinqueloculina* (%), suboxic genus *Bulimina* (%), dysoxic genus *Globobulimina* (%) and productivity indicator

$\delta^{13}C_{pf}$ also reveals a prominent ~23 kyr cyclicity that may be related to changes in KC intensity, as exhibited by the relative abundance of the KC indicator species *Globigerinoides ruber* at Site U1429 in the ECS. In addition, the ~23 kyr cyclicity likely reflects EAMS variability, which is modulated by precessional insolation. Thus, bottom water oxygen in the ECS is primarily regulated by primary marine productivity either through the nutrient influx from CDW discharge or the upwelling of nutrient-rich subsurface KC.

6 Conclusions

Multivariate analysis of benthic foraminiferal assemblages retraces the history and variability of ECS bottom water oxygenation over the last 400 kyr, suggesting four different phases of bottom water oxygenation. Bottom water was generally suboxic between mid MIS 11 and the end of MIS 8, except for transient intervals of suboxic to dysoxic conditions related to intermittent upwelling of subsurface Kuroshio water. The ECS bottom water subsequently became suboxic to dysoxic during MIS 7 and 6, reflecting a general increase in productivity and remained dysoxic for the remaining of MIS 5 and 4. Bottom water oxygenation exhibited major changes between oxic to dysoxic conditions from MIS 3 to 1. The dominant biofacies in the ECS over the last 400 kyr are biofacies Mc representing suboxic condition, biofacies Um representing suboxic to dysoxic condition and biofacies Co representing dysoxic conditions. The oxic benthic foraminifera and other marine productivity proxy $\delta^{13}C_{pf}$ respond to 100 kyr glacial-interglacial cycles. The oxic, suboxic, and dysoxic foraminifera genus and marine productivity proxy $\delta^{13}C_{pf}$ respond to 23 kyr precessional variability related to changes in EASM and KC strength. This study suggests that bottom water oxygenation in the ECS is directly influenced by primary marine productivity and by the terrigenous supply of organic matter on 100 and 23 kyr time scales.

Data Availability Statement

Benthic foraminiferal percentage abundance data for last 400 kyr from Site U1429 generated for this study. Major benthic foraminiferal abundance data, Biofacies abundance data and oxic-suboxic-dysoxic benthic foraminiferal species abundance data archived at Mendeley

Data (http://dx.doi.org/10.17632/gcsgc2byps.1; Vats et al., 2021, with closed access until acceptance).

Acknowledgments

The authors are grateful to IODP for providing core samples to RKS (Request No. #4201 and 13522). RKS, NV and DKP acknowledge the financial support given by the ESSO-National Centre for Polar and Ocean Research, Ministry of Earth Sciences, India, to carry this research (RP-077). NV acknowledges CSIR, New Delhi, for providing CSIR-JRF and CSIR-SRF (09/1059(0013)/2017-EMR-I). MD acknowledges DST, New Delhi, for providing INSPIRE Fellowship (IF150105). AKG thanks DST, New Delhi, for the J.C. Bose Fellowship (SR/S2/JCB-80/2011). Funding was provided by the Australian IODP Office and the Australian Research Council (ARC) Basins Genesis Hub (IH130200012) to SJG. The authors declare no conflicts of interest.

References

Akimoto, K., & Hasegawa, S. (1989). Bathymetric distribution of the Recent benthic foraminifers around Japan—As a contribution to the new paleobathymetric scale. *The Memoirs of the Geological Society of Japan*, *54*, 229–240.

Anderson, C. H., Murray, R. W., Dunlea, A. G., Giosan, L., Kinsley, C. W., McGee, D., & Tada, R. (2018). Climatically Driven Changes in the Supply of Terrigenous Sediment to the East China Sea. *Geochemistry, Geophysics, Geosystems*, *19*(8), 2463–2477. https://doi.org/10.1029/2017GC007339

Araújo, H. A. B. de, Dominguez, J. M. L., Machado, A. de J., & Rangel, A. G. de A. N. (2018). Benthic foraminifera distribution in a deltaic clinoform (São Francisco Delta, eastern Brazil): A reference study. *Journal of Marine Systems*, *186*, 1–16. https://doi.org/10.1016/j.jmarsys.2018.05.004

Balestra, B., Grunert, P., Ausin, B., Hodell, D., Flores, J.-A., Alvarez-Zarikian, C. A., et al. (2017). Coccolithophore and benthic foraminifera distribution patterns in the Gulf of Cadiz and Western Iberian Margin during Integrated Ocean Drilling Program (IODP) Expedition 339.

Journal of Marine Systems, *170*, 50–67. https://doi.org/10.1016/j.jmarsys.2017.01.005

Ballesteros-Prada, A. (2019). Modern Benthic Foraminifera "Phylum Foraminifera (D'Orbigny 1826)" of the Panama Bight: A Census Report Based on Thanatocoenoses from the Continental Slope. In G. Cusminsky, E. Bernasconi, G. Concheyro (Eds.) *Advances in South American Micropaleontology. Springer Earth System Sciences. Springer, Cham.* (pp. 175–213). https://doi.org/10.1007/978-3-030-02119-1_9

Barik, S. S., Singh, R. K., Jena, P. S., Tripathy, S., Sharma, K., & Prusty, P. (2019). Spatio-temporal variations in ecosystem and CO_2 sequestration in coastal lagoon: A foraminiferal perspective. *Marine Micropaleontology*, *147*, 43–56. https://doi.org/10.1016/j.marmicro.2019.02.003

Bernhard, J. M., Sen Gupta, B. K., & Borne, P. F. (1997). Benthic foraminiferal proxy to estimate dysoxic bottom-water oxygen concentrations; Santa Barbara Basin, U.S. Pacific continental margin. *The Journal of Foraminiferal Research*, *27*(4), 301–310. https://doi.org/10.2113/gsjfr.27.4.301

Bhaumik, A. K., Gupta, A. K., Sundar Raj, M., Mohan, K., De, S., & Sarkar, S. (2007). Paleoceanographic evolution of the northeastern Indian ocean during the Miocene: Evidence from deep-sea benthic foraminifera (DSDP Hole 216A). *Indian Journal of Marine Sciences*, *36*(4), 332–341.

Black, H. D., Anderson, W. T., & Alvarez Zarikian, C. A. (2018). Data report: organic matter, carbonate, and stable isotope stratigraphy from IODP Expedition 346 Sites U1426, U1427, and U1429. In R. Tada, et al., *Proceedings of the Integrated Ocean Drilling Program*, (Vol. 346). https://doi.org/10.2204/iodp.proc.346.204.2018

Bubenshchikova, N. V., Nürnberg, D., Gorbarenko, S. A., & Lembke-Jene, L. (2010). Variations of the oxygen minimum zone of the Okhotsk Sea during the last 50 ka as indicated by benthic foraminiferal and biogeochemical data. *Oceanology*, *50*(1), 93–106. https://doi.org/10.1134/S000143701001011X

Burkett, A. M., Rathburn, A. E., Elena Pérez, M., Levin, L. A., & Martin, J. B. (2016).

Colonization of over a thousand Cibicidoides wuellerstorfi (foraminifera: Schwager, 1866) on artificial substrates in seep and adjacent off-seep locations in dysoxic, deep-sea environments. *Deep Sea Research Part I: Oceanographic Research Papers*, *117*, 39–50. https://doi.org/10.1016/j.dsr.2016.08.011

Charrieau, L. M., Filipsson, H. L., Ljung, K., Chierici, M., Knudsen, K. L., & Kritzberg, E. (2018). The effects of multiple stressors on the distribution of coastal benthic foraminifera: A case study from the Skagerrak-Baltic Sea region. *Marine Micropaleontology*, *139*, 42–56. https://doi.org/10.1016/j.marmicro.2017.11.004

Chen, C. T. A., Ruo, R., Paid, S. C., Liu, C. T., & Wong, G. T. F. (1995). Exchange of water masses between the East China Sea and the Kuroshio off northeastern Taiwan. *Continental Shelf Research*, *15*(1), 19–39. https://doi.org/10.1016/0278-4343(93)E0001-O

Cheng, H., Edwards, R. L., Sinha, A., Spötl, C., Yi, L., Chen, S., et al. (2016). The Asian monsoon over the past 640,000 years and ice age terminations. *Nature*, *534*(7609), 640–646. https://doi.org/10.1038/nature18591

Clemens, S. C., Holbourn, A., Kubota, Y., Lee, K. E., Liu, Z., Chen, G., et al. (2018). Precession-band variance missing from East Asian monsoon runoff. *Nature Communications*, *9*(1), 3364. https://doi.org/10.1038/s41467-018-05814-0

Cronin, T. M., Seidenstein, J., Keller, K., McDougall, K., Ruefer, A., & Gemery, L. (2019). The benthic foraminifera Cassidulina from the Arctic Ocean: application to paleoceanography and biostratigraphy. *Micropaleontology*, *65*(2), 105–125.

Culver, S. J., & Buzas, M. A. (1980). Distribution of recent benthic foraminifera off the North American Atlantic coast. In *Smithsonian Contributions to the Marine Sciences*, (6), 1-512. https://doi.org/10.5479/si.01960768.6.1

Culver, S. J., & Buzas, M. A. (1987). Distribution of Recent benthic foraminifera off the Pacific coast of Mexico and Central America. In *Smithsonian Contributions to the Marine Sciences*, (30), 1–84. https://doi.org/10.5479/si.01960768.30.1

Das, Manisha, Singh, R. K., Holbourn, A., Farooq, S. H., Vats, N., & Pandey, D. K. (2021).

563 Paleoceanographic evolution of the Japan Sea during the Pleistocene – A benthic
564 foraminiferal perspective. *Palaeogeography, Palaeoclimatology, Palaeoecology*, *566*,
565 110238. https://doi.org/10.1016/j.palaeo.2021.110238

566 Das, Manisha, Singh, R. K., Vats, N., Holbourn, A., Mishra, S., Farooq, S. H., & Pandey, D. K.
567 (2018). Changes in the distribution of Uvigerinidae species over the past 775 kyr:
568 Implications for the paleoceanographic evolution of the Japan Sea. *Palaeogeography,*
569 *Palaeoclimatology, Palaeoecology*, *507*, 201–213.
570 https://doi.org/10.1016/j.palaeo.2018.07.019

571 Das, Manisha, Vats, N., Singh, R. K., Mishra, S., Barik, S. S., Divya, R. V., et al. (2020). Assessing
572 Mid-pleistocene to Holocene Sea-Ice Extent and Carbonate Compensation Depth
573 Fluctuations in the Japan Sea: A Multiproxy Approach. In D. Pandey, M. Ravichandran, N.
574 Nair, (Eds.) *Dynamics of the Earth System: Evolution, Processes and Interactions. Society of*
575 *Earth Scientists Series. Springer, Cham* (pp. 55–72). https://doi.org/10.1007/978-3-030-
576 40659-2_3

577 Das, Moumita, Singh, R. K., Gupta, A. K., & Bhaumik, A. K. (2017). Holocene strengthening of
578 the Oxygen Minimum Zone in the northwestern Arabian Sea linked to changes in
579 intermediate water circulation or Indian monsoon intensity? *Palaeogeography,*
580 *Palaeoclimatology, Palaeoecology*, *483*, 125–135.
581 https://doi.org/10.1016/j.palaeo.2016.10.035

582 De, S., & Gupta, A. K. (2010). Deep-sea faunal provinces and their inferred environments in the
583 Indian Ocean based on distribution of Recent benthic foraminifera. *Palaeogeography,*
584 *Palaeoclimatology, Palaeoecology*, *291*(3–4), 429–442.
585 https://doi.org/10.1016/j.palaeo.2010.03.012

586 Diz, P., & Francés, G. (2008). Distribution of live benthic foraminifera in the Ría de Vigo (NW
587 Spain). *Marine Micropaleontology*, *66*(3–4), 165–191.
588 https://doi.org/10.1016/j.marmicro.2007.09.001

589 Duros, P., Fontanier, C., Metzger, E., Pusceddu, A., Cesbron, F., de Stigter, H. C., et al. (2011).
590 Live (stained) benthic foraminifera in the Whittard Canyon, Celtic margin (NE Atlantic).

Deep Sea Research Part I: Oceanographic Research Papers, *58*(2), 128–146. https://doi.org/10.1016/j.dsr.2010.11.008

Fontanier, C., Jorissen, F. ., Licari, L., Alexandre, A., Anschutz, P., & Carbonel, P. (2002). Live benthic foraminiferal faunas from the Bay of Biscay: faunal density, composition, and microhabitats. *Deep Sea Research Part I: Oceanographic Research Papers*, *49*(4), 751–785. https://doi.org/10.1016/S0967-0637(01)00078-4

Fontanier, C., Jorissen, F. J., Chaillou, G., Anschutz, P., Grémare, A., & Griveaud, C. (2005). Live foraminiferal faunas from a 2800m deep lower canyon station from the Bay of Biscay: Faunal response to focusing of refractory organic matter. *Deep Sea Research Part I: Oceanographic Research Papers*, *52*(7), 1189–1227. https://doi.org/10.1016/j.dsr.2005.01.006

Fontanier, C., Jorissen, F. J., Lansard, B., Mouret, A., Buscail, R., Schmidt, S., et al. (2008). Live foraminifera from the open slope between Grand Rhône and Petit Rhône Canyons (Gulf of Lions, NW Mediterranean). *Deep Sea Research Part I: Oceanographic Research Papers*, *55*(11), 1532–1553. https://doi.org/10.1016/j.dsr.2008.07.003

Gallagher, S. J., Kitamura, A., Iryu, Y., Itaki, T., Koizumi, I., & Hoiles, P. W. (2015). The Pliocene to recent history of the Kuroshio and Tsushima Currents: a multi-proxy approach. *Progress in Earth and Planetary Science*, *2*(1), 17. https://doi.org/10.1186/s40645-015-0045-6

Gallagher, S. J., Sagawa, T., Henderson, A. C. G., Saavedra-Pellitero, M., De Vleeschouwer, D., Black, H., et al. (2018). East Asian Monsoon History and Paleoceanography of the Japan Sea Over the Last 460,000 Years. *Paleoceanography and Paleoclimatology*, *33*(7), 683–702. https://doi.org/10.1029/2018PA003331

Gallagher, S. J., Wallace, M. W., Li, C. L., Kinna, B., Bye, J. T., Akimoto, K., & Torii, M. (2009). Neogene history of the West Pacific Warm Pool, Kuroshio and Leeuwin currents. *Paleoceanography*, *24*(1), PA1206. https://doi.org/10.1029/2008PA001660

García-Sanz, I., Usera, J., Guillem, J., Giner-Baixauli, A., & Alberola, C. (2018). Geographical and bathymetric distribution of foraminiferal assemblages from the Alboran Sea (western Mediterranean). *Quaternary International*, *481*, 146–156.

https://doi.org/10.1016/j.quaint.2017.11.016

Garcia, H. E., Boyer, T. P., Locarnini, R. A., Antonov, J. I., Mishonov, A. V, Baranova, O. K., et al. (2013). *World Ocean Atlas 2013. Volume 3: dissolved oxygen, apparent oxygen utilization, and oxygen saturation*. NOAA Atlas NESDIS 75, 3, 27.

Gonzales, M. V., De Almeida, F. K., Costa, K. B., Santarosa, A. C. A., Camillo, E., De Quadros, J. P., & Toledo, F. A. L. (2017). Help index: Hoeglundina elegans preservation index for marine sediments in the western South Atlantic. *The Journal of Foraminiferal Research, 47*(1), 56–69. https://doi.org/10.2113/gsjfr.47.1.56

Gooday, A. J. (1988). A response by benthic Foraminifera to the deposition of phytodetritus in the deep sea. *Nature, 332*(6159), 70–73. https://doi.org/10.1038/332070a0

Gorbarenko, S. A., Southon, J. R., Keigwin, L. D., Cherepanova, M. V., & Gvozdeva, I. G. (2004). Late Pleistocene–Holocene oceanographic variability in the Okhotsk Sea: geochemical, lithological and paleontological evidence. *Palaeogeography, Palaeoclimatology, Palaeoecology, 209*(1–4), 281–301. https://doi.org/10.1016/j.palaeo.2004.02.013

Gorbarenko, S. A., Psheneva, O. Y., Artemova, A. V., Matul', A. G., Tiedemann, R., & Nürnberg, D. (2010). Paleoenvironment changes in the NW Okhotsk Sea for the last 18kyr determined with micropaleontological, geochemical, and lithological data. *Deep Sea Research Part I: Oceanographic Research Papers, 57*(6), 797–811. https://doi.org/10.1016/j.dsr.2010.04.004

Grunert, P., Rosenthal, Y., Jorissen, F., Holbourn, A., Zhou, X., & Piller, W. E. (2018). Mg/Ca-temperature calibration for costate Bulimina species (B. costata, B. inflata, B. mexicana): A paleothermometer for hypoxic environments. *Geochimica et Cosmochimica Acta, 220,* 36–54. https://doi.org/10.1016/j.gca.2017.09.021

Gupta, A. K., Sarkar, S., & Mukherjee, B. (2006). Paleoceanographic changes during the past 1.9 Myr at DSDP Site 238, Central Indian Ocean Basin: Benthic foraminiferal proxies. *Marine Micropaleontology*, *60*(2), 157–166. https://doi.org/10.1016/j.marmicro.2006.04.001

Gupta, A. K., Sundar Raj, M., Mohan, K., & De, S. (2008). A major change in monsoon-driven productivity in the tropical Indian Ocean during ca 1.2–0.9 Myr: Foraminiferal faunal and

stable isotope data. *Palaeogeography, Palaeoclimatology, Palaeoecology*, *261*(3–4), 234–245. https://doi.org/10.1016/j.palaeo.2008.01.012

Gupta, A. K., & Thomas, E. (1999). Latest Miocene-Pleistocene Productivity and Deep-Sea Ventilation in the Northwestern Indian Ocean (Deep Sea Drilling Project Site 219). *Paleoceanography*, *14*(1), 62–73. https://doi.org/10.1029/1998PA900006

Gupta, A. K., & Thomas, E. (2003). Initiation of Northern Hemisphere glaciation and strengthening of the northeast Indian monsoon: Ocean Drilling Program Site 758, eastern equatorial Indian Ocean. *Geology*, *31*(1), 47. https://doi.org/10.1130/0091-7613(2003)031<0047:IONHGA>2.0.CO;2

Haller, C., Hallock, P., Hine, A. C., & Smith, C. G. (2018). Benthic foraminifera from the Carnarvon Ramp reveal variability in Leeuwin Current activity (Western Australia) since the Pliocene. *Marine Micropaleontology*, *142*, 25–39. https://doi.org/10.1016/j.marmicro.2018.05.005

Hammer, O., Harper, D., & Ryan, P. D. (2001). PAST: paleontological statistic software package for education and data analyses. *Palaeontologia Electronica*, *4*.

Harloff, J., & Mackensen, A. (1997). Recent benthic foraminiferal associations and ecology of the Scotia Sea and Argentine Basin. *Marine Micropaleontology*, *31*(1–2), 1–29. https://doi.org/10.1016/S0377-8398(96)00059-X

Hayward, B. W., Grenfell, H., & Reid, C. (1997). Foraminiferal associations in Wanganui Bight and Queen Charlotte Sound, New Zealand. *New Zealand Journal of Marine and Freshwater Research*, *31*(3), 337–365. https://doi.org/10.1080/00288330.1997.9516771

Holbourn, A., Henderson, A. S., & MacLeod, N. (2013). *Atlas of Benthic Foraminifera*. Oxford, UK: Wiley-Blackwell. https://doi.org/10.1002/9781118452493

Hu, J., & Wang, X. H. (2016). Progress on upwelling studies in the China seas. *Reviews of Geophysics*, *54*(3), 653–673. https://doi.org/10.1002/2015RG000505

Huang, H.-H. M., Yasuhara, M., Iwatani, H., Yamaguchi, T., Yamada, K., & Mamo, B. (2019).

Deep-sea ostracod faunal dynamics in a marginal sea: biotic response to oxygen variability and mid-Pleistocene global changes. *Paleobiology*, *45*(1), 85–97. https://doi.org/10.1017/pab.2018.37

Ichikawa, H., & Beardsley, R. C. (2002). Review: the current system in the yellow and East China seas. *Journal of Oceanography*, *58*. https://doi.org/10.1023/A:1015876701363

Irino, T., Tada, R., Ikehara, K., Sagawa, T., Karasuda, A., Kurokawa, S., et al. (2018). Construction of perfectly continuous records of physical properties for dark-light sediment sequences collected from the Japan Sea during Integrated Ocean Drilling Program Expedition 346 and their potential utilities as paleoceanographic studies. *Progress in Earth and Planetary Science*, *5*(1), 23. https://doi.org/10.1186/s40645-018-0176-7

Jian, Z., Wang, L., Kienast, M., Sarnthein, M., Kuhnt, W., Lin, H., & Wang, P. (1999). Benthic foraminiferal paleoceanography of the South China Sea over the last 40,000 years. *Marine Geology*, *156*(1–4), 159–186. https://doi.org/10.1016/S0025-3227(98)00177-7

Jones, R. W., & Brady, H. B. (1994). *The challenger foraminifera*. Oxford University Press, USA.

Joos, F., Plattner, G.-K., Stocker, T. F., Körtzinger, A., & Wallace, D. W. R. (2003). Trends in marine dissolved oxygen: Implications for ocean circulation changes and the carbon budget. *Eos, Transactions American Geophysical Union*, *84*(21), 197. https://doi.org/10.1029/2003EO210001

Jorissen, F. J., Wittling, I., Peypouquet, J. P., Rabouille, C., & Relexans, J. C. (1998). Live benthic foraminiferal faunas off Cape Blanc, NW-Africa: Community structure and microhabitats. *Deep Sea Research Part I: Oceanographic Research Papers*, *45*(12), 2157–2188. https://doi.org/10.1016/S0967-0637(98)00056-9

Jorissen, F. J., Fontanier, C., & Thomas, E. (2007). Chapter Seven Paleoceanographical Proxies Based on Deep-Sea Benthic Foraminiferal Assemblage Characteristics. In *Developments in Marine Geology* (pp. 263–325). https://doi.org/10.1016/S1572-5480(07)01012-3

Kaiho, K., & Nishimura, A. (1992). Distribution of Holocene Benthic Foraminifers in the Izu-Bonin Arc. In B. Taylor, et al., *Proceedings of the Ocean Drilling Program, Scientific Results*

(Vol. 126, pp. 311–320). Ocean Drilling Program. https://doi.org/10.2973/odp.proc.sr.126.138.1992

Kaiho, K. (1994). Benthic foraminiferal dissolved-oxygen index and dissolved-oxygen levels in the modern ocean. *Geology*, *22*(8), 719. https://doi.org/10.1130/0091-7613(1994)022<0719:BFDOIA>2.3.CO;2

Kaiho, K. (1999). Effect of organic carbon flux and dissolved oxygen on the benthic foraminiferal oxygen index (BFOI). *Marine Micropaleontology*, *37*(1), 67–76. https://doi.org/10.1016/S0377-8398(99)00008-0

Kaminski, M. A. (2012). Calibration of the Benthic Foraminiferal Oxygen Index in the Marmara Sea. *Geological Quarterly*, *56*(4), 757–756. https://doi.org/10.7306/gq.1061

Kastens, K., & Mascle, J. (1990). The Geological Evolution of the Tyrrhenian Sea: An Introduction to the Scientific Results of ODP Leg 107. In K. A. Kastens,, et al., *Proceedings of the Ocean Drilling Program, Scientific Results* (Vol. 107, pp. 3–26). Ocean Drilling Program. https://doi.org/10.2973/odp.proc.sr.107.187.1990

Kender, S., & Kaminski, M. A. (2017). Modern deep-water agglutinated foraminifera from IODP Expedition 323, Bering Sea: ecological and taxonomic implications. *Journal of Micropalaeontology*, 195–218. https://doi.org/10.1144/jmpaleo2016-026

Kido, Y., Minami, I., Tada, R., Fujine, K., Irino, T., Ikehara, K., & Chun, J.-H. (2007). Orbital-scale stratigraphy and high-resolution analysis of biogenic components and deep-water oxygenation conditions in the Japan Sea during the last 640 kyr. *Palaeogeography, Palaeoclimatology, Palaeoecology*, *247*(1–2), 32–49. https://doi.org/10.1016/j.palaeo.2006.11.020

Kubota, Y., Kimoto, K., Tada, R., Oda, H., Yokoyama, Y., & Matsuzaki, H. (2010). Variations of East Asian summer monsoon since the last deglaciation based on Mg/Ca and oxygen isotope of planktic foraminifera in the northern East China Sea. *Paleoceanography*, *25*(4), PA4205. https://doi.org/10.1029/2009PA001891

Kubota, Y., Kimoto, K., Tada, R., Uchida, M., & Ikehara, K. (2019). Millennial-scale variability

of East Asian summer monsoon inferred from sea surface salinity in the northern East China Sea (ECS) and its impact on the Japan Sea during Marine Isotope Stage (MIS) 3. *Progress in Earth and Planetary Science*, *6*(1), 39. https://doi.org/10.1186/s40645-019-0283-0

Kuhnt, W., Hess, S., & Jian, Z. (1999). Quantitative composition of benthic foraminiferal assemblages as a proxy indicator for organic carbon flux rates in the South China Sea. *Marine Geology*, *156*(1–4), 123–157. https://doi.org/10.1016/S0025-3227(98)00176-5

Laprida, C., Chapori, N. G., Violante, R. A., & Compagnucci, R. H. (2007). Mid-Holocene evolution and paleoenvironments of the shoreface–offshore transition, north-eastern Argentina: New evidence based on benthic microfauna. *Marine Geology*, *240*(1–4), 43–56. https://doi.org/10.1016/j.margeo.2007.02.001

Lee, T. N., Johns, W. E., Liu, C.-T., Zhang, D., Zantopp, R., & Yang, Y. (2001). Mean transport and seasonal cycle of the Kuroshio east of Taiwan with comparison to the Florida Current. *Journal of Geophysical Research: Oceans*, *106*(C10), 22143–22158. https://doi.org/10.1029/2000JC000535

Levin, L. A. (2002). Deep-Ocean Life Where Oxygen Is Scarce: Oxygen-deprived zones are common and might become more so with climate change. Here life hangs on, with some unusual adaptations. *American Scientist*, *90*(5), 436–444.

Liu, K.-K., Gong, G.-C., Lin, S., Yang, C.-Y., Wei, C.-L., Pai, S.-C., & Wu, C.-K. (1992). The Year-Round Upwelling at the Shelf Break Near the Northern Tip of Taiwan as Evidenced by Chemical Hydrography. *Terrestrial, Atmospheric and Oceanic Sciences*, *3*(3), 243–276. https://doi.org/10.3319/TAO.1992.3.3.243(KEEP)

Locarnini, R. A., Mishonov, A. V., Baranova, O. K., Boyer, T. P., Zweng, M. M., Garcia, H. E., et al. (2019). *World Ocean Atlas 2018. Volume 1 : Temperature*. NOAA Atlas NESDIS 81, 1, 52.

Loeblich, A. R., & Tappan, H. (1988). *Foraminiferal Genera and Their Classification*. Boston, MA: Springer US. https://doi.org/10.1007/978-1-4899-5760-3

Lutze, G. F. (1979). Benthic Foraminifers at Site 397: Faunal Fluctuations and Ranges in the

Quaternary. In *Initial Reports of the Deep Sea Drilling Project, 47 Pt. 1* (pp. 419–431). https://doi.org/10.2973/dsdp.proc.47-1.111.1979

Lutze, G. F., & Thiel, H. (1989). Epibenthic foraminifera from elevated microhabitats; Cibicidoides wuellerstorfi and Planulina ariminensis. *The Journal of Foraminiferal Research, 19*(2), 153–158. https://doi.org/10.2113/gsjfr.19.2.153

Ma, R., Sépulcre, S., Licari, L., Bassinot, F., Liu, Z., Tisnérat-Laborde, N., et al. (2019). Changes in Intermediate Circulation in the Bay of Bengal Since the Last Glacial Maximum as Inferred From Benthic Foraminifera Assemblages and Geochemical Proxies. *Geochemistry, Geophysics, Geosystems*, *20*(3), 1592–1608. https://doi.org/10.1029/2018GC008179

Mackensen, A., & Hald, M. (1988). Cassidulina teretis Tappan and C. laevigata d'Orbigny; their modern and late Quaternary distribution in northern seas. *The Journal of Foraminiferal Research*, *18*(1), 16–24. https://doi.org/10.2113/gsjfr.18.1.16

Mackensen, A., Schmiedl, G., Harloff, J., & Giese, M. (1995). Deep-sea foraminifera in the South Atlantic ocean: Ecology and assemblage generation. *Micropaleontology*, *41*(4), 342–358. https://doi.org/10.2307/1485808

Martínez-García, B., Pascual, A., Rodríguez-Lázaro, J., & Bodego, A. (2013). Recent benthic foraminifers of the Basque continental shelf (Bay of Biscay, northern Spain): Oceanographic implications. *Continental Shelf Research*, *66*, 105–122. https://doi.org/10.1016/j.csr.2013.07.006

Martins, V., Dubert, J., Jouanneau, J.-M., Weber, O., da Silva, E. F., Patinha, C., et al. (2007). A multiproxy approach of the Holocene evolution of shelf–slope circulation on the NW Iberian Continental Shelf. *Marine Geology*, *239*(1–2), 1–18. https://doi.org/10.1016/j.margeo.2006.11.001

Matsuzaki, K. M., Itaki, T., & Kimoto, K. (2016). Vertical distribution of polycystine radiolarians in the northern East China Sea. *Marine Micropaleontology*, *125*, 66–84. https://doi.org/10.1016/j.marmicro.2016.03.004

Matsuzaki, K. M., Itaki, T., & Tada, R. (2019). Paleoceanographic changes in the Northern East

China Sea during the last 400 kyr as inferred from radiolarian assemblages (IODP Site U1429). *Progress in Earth and Planetary Science*, *6*(1), 22. https://doi.org/10.1186/s40645-019-0256-3

Mazumder, A., & Nigam, R. (2014). Bathymetric preference of four major genera of rectilinear benthic foraminifera within oxygen minimum zone in Arabian Sea off central west coast of India. *Journal of Earth System Science*, *123*(3), 633–639. https://doi.org/10.1007/s12040-014-0419-y

McGann, M., & Conrad, J. E. (2018). Faunal and stable isotopic analyses of benthic foraminifera from the Southeast Seep on Kimki Ridge offshore southern California, USA. *Deep Sea Research Part II: Topical Studies in Oceanography*, *150*, 92–117. https://doi.org/10.1016/j.dsr2.2018.01.011

Murray, J. W. (2006). Ecology and Applications of Benthic Foraminifera. In *Ecology and applications of benthic foraminifera,Cambridge University Press*. Cambridge: Cambridge University Press. https://doi.org/10.1017/CBO9780511535529

Nardelli, M. P., Barras, C., Metzger, E., Mouret, A., Filipsson, H. L., Jorissen, F., & Geslin, E. (2014). Experimental evidence for foraminiferal calcification under anoxia. *Biogeosciences*, *11*(14), 4029–4038. https://doi.org/10.5194/bg-11-4029-2014

Pascual, A., Rodríguez-Lázaro, J., Martínez-García, B., & Varela, Z. (2020). Palaeoceanographic and palaeoclimatic changes during the last 37,000 years detected in the SE Bay of Biscay based on benthic foraminifera. *Quaternary International*, *566–567*, 323–336. https://doi.org/10.1016/j.quaint.2020.03.043

Patarroyo, G. D., & Martínez, J. I. (2015). Late quaternary sea bottom conditions in the southern Panama basin, Eastern Equatorial Pacific. *Journal of South American Earth Sciences*, *63*, 346–359. https://doi.org/10.1016/j.jsames.2015.07.010

Pérez-Asensio, J. N., Aguirre, J., & Rodríguez-Tovar, F. J. (2017). The effect of bioturbation by polychaetes (Opheliidae) on benthic foraminiferal assemblages and test preservation. *Palaeontology*, *60*(6), 807–827. https://doi.org/10.1111/pala.12317

Phleger, F. B., & Soutar, A. (1973). Production of Benthic Foraminifera in Three East Pacific Oxygen Minima. *Micropaleontology*, *19*(1), 110. https://doi.org/10.2307/1484973

Rathburn, A. E., & Corliss, B. H. (1994). The ecology of living (stained) deep-sea benthic foraminifera from the Sulu Sea. *Paleoceanography*, *9*(1), 87–150. https://doi.org/10.1029/93PA02327

Rathburn, A. E., Willingham, J., Ziebis, W., Burkett, A. M., & Corliss, B. H. (2018). A New biological proxy for deep-sea paleo-oxygen: Pores of epifaunal benthic foraminifera. *Scientific Reports*, *8*(1), 9456. https://doi.org/10.1038/s41598-018-27793-4

Reolid, M., Rodríguez-Tovar, F. J., & Nagy, J. (2012). Ecological replacement of Valanginian agglutinated foraminifera during a maximum flooding event in the Boreal realm (Spitsbergen). *Cretaceous Research*, *33*(1), 196–204. https://doi.org/10.1016/j.cretres.2011.10.003

Revelle, W. (2019). *psych: Procedures for Psychological, Psychometric, and Personality Research.* Northwestern University, Evanston, Illinois. R package version 1.9.12, https://cran.r-project.org/package=psych.

Rostami, M. A., Frontalini, F., Leckie, R. M., Coccioni, R., Font, E., & Balmaki, B. (2020). Benthic Foraminifera Across the Cretaceous/Paleogene Boundary in the Eastern Tethys (Northern Alborz, Galanderud Section): Extinction Pattern and Paleoenvironmental Reconstruction. *Journal of Foraminiferal Research*, *50*(1), 25–40. https://doi.org/10.2113/gsjfr.50.1.25

RStudio Team. (2020). *RStudio: Integrated Development Environment for R*. Boston, MA. http://www.rstudio.com/

Ryan, W. B. F., Carbotte, S. M., Coplan, J. O., O'Hara, S., Melkonian, A., Arko, R., et al. (2009). Global Multi-Resolution Topography synthesis. *Geochemistry, Geophysics, Geosystems*, *10*(3), Q03014. https://doi.org/10.1029/2008GC002332

Saavedra-Pellitero, M., Baumann, K.-H., Gallagher, S. J., Sagawa, T., & Tada, R. (2019). Paleoceanographic evolution of the Japan Sea over the last 460 kyr – A coccolithophore

perspective. *Marine Micropaleontology*, *152*, 101720. https://doi.org/10.1016/j.marmicro.2019.01.001

Sagawa, T., Nagahashi, Y., Satoguchi, Y., Holbourn, A., Itaki, T., Gallagher, S. J., et al. (2018). Integrated tephrostratigraphy and stable isotope stratigraphy in the Japan Sea and East China Sea using IODP Sites U1426, U1427, and U1429, Expedition 346 Asian Monsoon. *Progress in Earth and Planetary Science*, *5*(1), 18. https://doi.org/10.1186/s40645-018-0168-7

Saravanan, P., Gupta, A. K., Zheng, H., Panigrahi, M. K., & Prakasam, M. (2019). Late Holocene long arid phase in the Indian subcontinent as seen in shallow sediments of the eastern Arabian Sea. *Journal of Asian Earth Sciences*, *181*, 103915. https://doi.org/10.1016/j.jseaes.2019.103915

Sarkar, S., & Gupta, A. K. (2014). Late Quaternary productivity changes in the equatorial Indian Ocean (ODP Hole 716A). *Palaeogeography, Palaeoclimatology, Palaeoecology*, *397*, 7–19. https://doi.org/10.1016/j.palaeo.2013.12.002

Schmiedl, G., Mackensen, A., & Müller, P. J. (1997). Recent benthic foraminifera from the eastern South Atlantic Ocean: Dependence on food supply and water masses. *Marine Micropaleontology*, *32*(3–4), 249–287. https://doi.org/10.1016/S0377-8398(97)00023-6

Schmiedl, G, de Bovée, F., Buscail, R., Charrière, B., Hemleben, C., Medernach, L., & Picon, P. (2000). Trophic control of benthic foraminiferal abundance and microhabitat in the bathyal Gulf of Lions, western Mediterranean Sea. *Marine Micropaleontology*, *40*(3), 167–188. https://doi.org/10.1016/S0377-8398(00)00038-4

Schmiedl, G., & Leuschner, D. C. (2005). Oxygenation changes in the deep western Arabian Sea during the last 190,000 years: Productivity versus deepwater circulation. *Paleoceanography*, *20*(2), PA2008. https://doi.org/10.1029/2004PA001044

Schmiedl, G., & Mackensen, A. (1997). Late Quaternary paleoproductivity and deep water circulation in the eastern South Atlantic Ocean: Evidence from benthic foraminifera. *Palaeogeography, Palaeoclimatology, Palaeoecology*, *130*(1–4), 43–80. https://doi.org/10.1016/S0031-0182(96)00137-X

Schulz, M., & Mudelsee, M. (2002). REDFIT: estimating red-noise spectra directly from unevenly spaced paleoclimatic time series. *Computers & Geosciences*, *28*(3), 421–426. https://doi.org/10.1016/S0098-3004(01)00044-9

Schweizer, M. (2006). *Evolution and molecular phylogeny of Cibicides and Uvigerina (Rotalida, Foraminifera)*. Utrecht University.

Scott, D. B., Schell, T., Rochon, A., & Blasco, S. (2008). Modern benthic foraminifera in the surface sediments of the Beaufort shelf, slope and Mackenzie trough, Beaufort sea, Canada: taxonomy and summary of surficial distributions. *The Journal of Foraminiferal Research*, *38*(3), 228–250. https://doi.org/10.2113/gsjfr.38.3.228

Scott, D. B., Takayanagi, Y., Hasegawa, S., & Saito, T. (2000). Illustration and taxonomic reevaluation of neogene foraminifera described from Japan. *Palaeontologia Electronica*, *3*(2), 1–41.

Sen Gupta, B. K., & Machain-Castillo, M. L. (1993). Benthic foraminifera in oxygen-poor habitats. *Marine Micropaleontology*, *20*(3–4), 183–201. https://doi.org/10.1016/0377-8398(93)90032-S

Shannon, C. E., & Weaver, W. (1949). *The mathematical theory of communication*. Urbana: University of Illinois Press.

Singh, A. D., Rai, A. K., Tiwari, M., Naidu, P. D., Verma, K., Chaturvedi, M., et al. (2015). Fluctuations of Mediterranean Outflow Water circulation in the Gulf of Cadiz during MIS 5 to 7: Evidence from benthic foraminiferal assemblage and stable isotope records. *Global and Planetary Change*, *133*, 125–140. https://doi.org/10.1016/j.gloplacha.2015.08.005

Singh, R. K., & Gupta, A. K. (2004). Late Oligocene–Miocene paleoceanographic evolution of the southeastern Indian Ocean: evidence from deep-sea benthic foraminifera (ODP Site 757). *Marine Micropaleontology*, *51*(1–2), 153–170. https://doi.org/10.1016/j.marmicro.2003.10.003

Singh, R. K., & Gupta, A. K. (2010). Deep-sea benthic foraminiferal changes in the eastern Indian Ocean (ODP Hole 757B): Their links to deep Indonesian (Pacific) flow and high latitude

glaciation during the Neogene. *Episodes, International Union of Geological Sciences*, *33*(2), 74–82. https://doi.org/10.18814/epiiugs/2010/v33i2/001

Smith, P. B. (1964). Ecology of benthonic species. *Geological Survey Professional Paper*, *429-B*, B1–B55.

Tada, R., Murray, R. W., Alvarez Zarikian, C. A., Anderson, W. T. J., Bassetti, M.-A., Brace, B. J., et al. (2015). Sites U1428 and U1429. In *Proceedings of the Integrated Ocean Drilling Program*, (Vol. 346). https://doi.org/10.2204/iodp.proc.346.109.2015

Tada, R., Irino, T., & Koizumi, I. (1999). Land-ocean linkages over orbital and millennial timescales recorded in Late Quaternary sediments of the Japan Sea. *Paleoceanography*, *14*(2), 236–247. https://doi.org/10.1029/1998PA900016

Takata, H., Kim, H. J., Asahi, H., Thomas, E., Yoo, C. M., Chi, S. B., & Khim, B.-K. (2019). Central Equatorial Pacific benthic foraminifera during the mid-Brunhes dissolution interval: Ballasting of particulate organic matter by biogenic silica and carbonate. *Quaternary Science Reviews*, *210*, 64–79. https://doi.org/10.1016/j.quascirev.2019.02.030

Takata, H., Nishida, N., Ikehara, K., Katsuki, K., & Khim, B.-K. (2018). Mid-Holocene forcing of the Tsushima Warm Current to the coastal environments in southwestern Japan with a view to foraminiferal faunas. *Quaternary International*, *482*, 56–66. https://doi.org/10.1016/j.quaint.2018.04.024

Taylor, M. A., Hendy, I. L., & Chappaz, A. (2017). Assessing oxygen depletion in the Northeastern Pacific Ocean during the last deglaciation using I/Ca ratios from multiple benthic foraminiferal species. *Paleoceanography*, *32*(8), 746–762. https://doi.org/10.1002/2016PA003062

Van Morkhoven, F. P. C. M., Berggren, W. A., Edwards, A. S., & Oertli, H. J. (1986). *Cenozoic cosmopolitan deep-water benthic Foraminifera*. Pau: Elf Aquitaine.

Vats, N., Mishra, S., Singh, R. K., Gupta, A. K., & Pandey, D. K. (2020). Paleoceanographic changes in the East China Sea during the last ~400 kyr reconstructed using planktic foraminifera. *Global and Planetary Change*, 103173.

https://doi.org/10.1016/j.gloplacha.2020.103173

Vats, N., Singh, R. K., Das, M., Holbourn, A., Gupta, A. K., Gallagher, S. J., & Pandey, D. K. (2021). Linkages between East China Sea Deep-sea Oxygenation and the Variability of the East Asian Summer Monsoon and Kuroshio Current over last 400,000 years [Data Set]. *Mendeley Data*, V1. http://dx.doi.org/10.17632/gcsgc2byps.1

Verma, S., Gupta, A. K., & Singh, R. K. (2013). Variations in deep-sea benthic foraminifera at ODP Hole 756B, southeastern Indian Ocean: Evidence for changes in deep ocean circulation. *Palaeogeography, Palaeoclimatology, Palaeoecology*, *376*, 172–183. https://doi.org/10.1016/j.palaeo.2013.02.034

Wang, N., Huang, B.-Q., Dong, Y.-T., & Xie, X. (2018). The evolution of deepwater dissolved oxygen in the northern South China Sea since 400 ka. *Palaeoworld*, *27*(2), 301–308. https://doi.org/10.1016/j.palwor.2017.11.001

Watanabe, S., Tada, R., Ikehara, K., Fujine, K., & Kido, Y. (2007). Sediment fabrics, oxygenation history, and circulation modes of Japan Sea during the Late Quaternary. *Palaeogeography, Palaeoclimatology, Palaeoecology*, *247*(1–2), 50–64. https://doi.org/10.1016/j.palaeo.2006.11.021

Wu, C.-R., Lu, H.-F., & Chao, S.-Y. (2008). A numerical study on the formation of upwelling off northeast Taiwan. *Journal of Geophysical Research*, *113*(C8), C08025. https://doi.org/10.1029/2007JC004697

Yamamoto, A., Abe-Ouchi, A., Shigemitsu, M., Oka, A., Takahashi, K., Ohgaito, R., & Yamanaka, Y. (2015). Global deep ocean oxygenation by enhanced ventilation in the Southern Ocean under long-term global warming. *Global Biogeochemical Cycles*, *29*(10), 1801–1815. https://doi.org/10.1002/2015GB005181

Zhao, B., Yan, X., Wang, Z., Shi, Y., Chen, Z., Xie, J., et al. (2018). Sedimentary evolution of the Yangtze River mouth (East China Sea) over the past 19,000 years, with emphasis on the Holocene variations in coastal currents. *Palaeogeography, Palaeoclimatology, Palaeoecology*, *490*, 431–449. https://doi.org/10.1016/j.palaeo.2017.11.023

941 Zhao, D., Wan, S., Song, Z., Gong, X., Zhai, L., Shi, X., & Li, A. (2019). Asynchronous Variation
942 in the Quaternary East Asian Winter Monsoon Associated With the Tropical Pacific ENSO-
943 Like System. *Geophysical Research Letters*, *46*(12), 6955–6963.
944 https://doi.org/10.1029/2019GL083033

945 Zhao, D., Wan, S., Toucanne, S., Clift, P. D., Tada, R., Révillon, S., et al. (2017). Distinct control
946 mechanism of fine-grained sediments from Yellow River and Kyushu supply in the northern
947 Okinawa Trough since the last glacial. *Geochemistry, Geophysics, Geosystems*, *18*(8), 2949–
948 2969. https://doi.org/10.1002/2016GC006764

949 Zhou, P., Song, X., Yuan, Y., Cao, X., Wang, W., Chi, L., & Yu, Z. (2018). Water Mass Analysis
950 of the East China Sea and Interannual Variation of Kuroshio Subsurface Water Intrusion
951 Through an Optimum Multiparameter Method. *Journal of Geophysical Research: Oceans*,
952 *123*(5), 3723–3738. https://doi.org/10.1029/2018JC013882

953 Zhou, Y., Chen, F., Wu, C., Yu, S., & Zhuang, C. (2016). Palaeoproductivity linked to monsoon
954 variability in the northern slope of the South China Sea from the last 290 kyr: evidence of
955 benthic foraminifera from Core SH7B. *Geological Society, London, Special Publications*,
956 *429*(1), 197–210. https://doi.org/10.1144/SP429.10

957 Zwaan, G. J. van der, Jorissen, F. J., Verhallen, P. J. J. M., & Daniels, C. H. von. (1986). Atlantic-
958 European oligocene to recent uvigerina : taxonomy, paleoecology and paleobiogeography.
959 *Utrecht Micropaleontological Bulletins*, *35*.

960 Zweng, M. M., Reagan, J. R., Seidov, D., Boyer, T. P., Antonov, J. I., Locarnini, R. A., et al.
961 (2019). *World Ocean Atlas 2018, Volume 2: Salinity*. NOAA Atlas NESDIS 82, 2, 50.